

EUR 3321.e

EUROPEAN ATOMIC ENERGY COMMUNITY - EURATOM

INFLUENCE OF NITROGEN
IN IRON AND STEEL
UNDER FAST NEUTRON IRRADIATION

by

S. APPIANO*, M. CASTAGNA*, A. FERRO**, G. MONTALENTI**,
A. A. ROSSI*, F. S. ROSSI*, M. ROSSI* and G. P. SOARDO**

*SORIN

**IENGF - Istituto Elettrotecnico Nazionale Galileo Ferraris, Torino

1967



EURATOM/US Agreement for Cooperation
EURAE C Report No. 1773 prepared by SORIN
Centro Ricerche Nucleari, Saluggia - Italy
Euratom Contract No. 074-65-10 TEEI

LEGAL NOTICE

This document was prepared under the sponsorship of the Commission of the European Atomic Energy Community (Euratom) in pursuance of the joint programme laid down by the Agreement for Cooperation signed on 8 November 1958 between the Government of the United States of America and the European Atomic Energy Community.

It is specified that neither the Euratom Commission, nor the Government of the United States, their contractors or any person acting on their behalf :

Make any warranty or representation, express or implied, with respect to the accuracy, completeness, or usefulness of the information contained in this document, or that the use of any information, apparatus, method, or process disclosed in this document may not infringe privately owned rights ; or

Assume any liability with respect to the use of, or for damages resulting from the use of any information, apparatus, method or process disclosed in this document.

This report is on sale at the addresses listed on cover page 4

at the price of FF 10.—	FB 100	DM 8.—	Lit. 1250	Fl. 7.25
-------------------------	--------	--------	-----------	----------

When ordering, please quote the EUR number and the title, which are indicated on the cover of each report.

Printed by L. Vannelle N.V.
Brussels, May 1967

This document was reproduced on the basis of the best available copy.

EUR 3321.e

INFLUENCE OF NITROGEN IN IRON AND STEEL UNDER FAST NEUTRON IRRADIATION by S. APPIANO*, M. CASTAGNA*, A. FERRO**, G. MONTALENTI**, A.A. ROSSI*, F.S. ROSSI*, M. ROSSI* and G.P. SOARDO**

* SORIN

** IENGF — Istituto Elettrotecnico Nazionale Galileo Ferraris, Torino

European Atomic Energy Community — EURATOM
EURATOM/US Agreement for Cooperation
EURAEK Report No. 1773 prepared by SORIN
Centro Ricerche Nucleari, Saluggia (Italy)
Euratom Contract No. 074-65-10 TEEI
Brussels, May 1967 — 70 Pages — 50 Figures — FB 100

The report is divided into three chapters dealing with the work done in different sections of the research :

a) Properties of iron alloys ; it summarizes the results attained with

EUR 3321.e

INFLUENCE OF NITROGEN IN IRON AND STEEL UNDER FAST NEUTRON IRRADIATION by S. APPIANO*, M. CASTAGNA*, A. FERRO**, G. MONTALENTI**, A.A. ROSSI*, F.S. ROSSI*, M. ROSSI* and G.P. SOARDO**

* SORIN

** IENGF — Istituto Elettrotecnico Nazionale Galileo Ferraris, Torino

European Atomic Energy Community — EURATOM
EURATOM/US Agreement for Cooperation
EURAEK Report No. 1773 prepared by SORIN
Centro Ricerche Nucleari, Saluggia (Italy)
Euratom Contract No. 074-65-10 TEEI
Brussels, May 1967 — 70 Pages — 50 Figures — FB 100

The report is divided into three chapters dealing with the work done in different sections of the research :

a) Properties of iron alloys ; it summarizes the results attained with

EUR 3321.e

INFLUENCE OF NITROGEN IN IRON AND STEEL UNDER FAST NEUTRON IRRADIATION by S. APPIANO*, M. CASTAGNA*, A. FERRO**, G. MONTALENTI**, A.A. ROSSI*, F.S. ROSSI*, M. ROSSI* and G.P. SOARDO**

* SORIN

** IENGF — Istituto Elettrotecnico Nazionale Galileo Ferraris, Torino

European Atomic Energy Community — EURATOM
EURATOM/US Agreement for Cooperation
EURAEK Report No. 1773 prepared by SORIN
Centro Ricerche Nucleari, Saluggia (Italy)
Euratom Contract No. 074-65-10 TEEI
Brussels, May 1967 — 70 Pages — 50 Figures — FB 100

The report is divided into three chapters dealing with the work done in different sections of the research :

a) Properties of iron alloys ; it summarizes the results attained with

tensile tests, impact tests, fracture surface analysis and magnetic measurements on pure iron or low alloyed iron. Some details are also given about the facilities set up for the damage recovery studies and for the irradiation of the specimens at controlled temperature.

- b) Neutron spectrum influence studies. The first data are quoted dealing with the works begun in order to give better information about the irradiation conditions. Neutron fluence data have been so far reported as > 1 MeV values : with the present work a better correlation with the spectrum shape will be attempted taking into account the literature references. Magnetic and mechanical properties of specimens irradiated in different reactor positions will be tested : the irradiation facilities and the specimens set up are briefly described.
- c) Properties of some ASTM 212 type steels killed with Si, Al or Ti. New tests have been done to evaluate the transition temperature of these materials and a structure analysis has been also done in different heat treatment conditions.

tensile tests, impact tests, fracture surface analysis and magnetic measurements on pure iron or low alloyed iron. Some details are also given about the facilities set up for the damage recovery studies and for the irradiation of the specimens at controlled temperature.

- b) Neutron spectrum influence studies. The first data are quoted dealing with the works begun in order to give better information about the irradiation conditions. Neutron fluence data have been so far reported as > 1 MeV values : with the present work a better correlation with the spectrum shape will be attempted taking into account the literature references. Magnetic and mechanical properties of specimens irradiated in different reactor positions will be tested : the irradiation facilities and the specimens set up are briefly described.
- c) Properties of some ASTM 212 type steels killed with Si, Al or Ti. New tests have been done to evaluate the transition temperature of these materials and a structure analysis has been also done in different heat treatment conditions.

tensile tests, impact tests, fracture surface analysis and magnetic measurements on pure iron or low alloyed iron. Some details are also given about the facilities set up for the damage recovery studies and for the irradiation of the specimens at controlled temperature.

- b) Neutron spectrum influence studies. The first data are quoted dealing with the works begun in order to give better information about the irradiation conditions. Neutron fluence data have been so far reported as > 1 MeV values : with the present work a better correlation with the spectrum shape will be attempted taking into account the literature references. Magnetic and mechanical properties of specimens irradiated in different reactor positions will be tested : the irradiation facilities and the specimens set up are briefly described.
- c) Properties of some ASTM 212 type steels killed with Si, Al or Ti. New tests have been done to evaluate the transition temperature of these materials and a structure analysis has been also done in different heat treatment conditions.

EUR 3321.e

EUROPEAN ATOMIC ENERGY COMMUNITY - EURATOM

INFLUENCE OF NITROGEN
IN IRON AND STEEL
UNDER FAST NEUTRON IRRADIATION

by

S. APPIANO*, M. CASTAGNA*, A. FERRO**, G. MONTALENTI**,
A. A. ROSSI*, F. S. ROSSI*, M. ROSSI* and G. P. SOARDO**

*SORIN

**IENGF - Istituto Elettrotecnico Nazionale Galileo Ferraris, Torino

1967



EURATOM/US Agreement for Cooperation
EURAEK Report No. 1773 prepared by SORIN
Centro Ricerche Nucleari, Saluggia - Italy
Euratom Contract No. 074-65-10 TEEI

SUMMARY

The report is divided into three chapters dealing with the work done in different sections of the research :

- a) Properties of iron alloys ; it summarizes the result attained with tensile tests, impact tests, fracture surface analysis and magnetic measurements on pure iron or low alloyed iron. Some details are also given about the facilities set up for the damage recovery studies and for the irradiation of the specimens at controlled temperature.
- b) Neutron spectrum influence studies. The first data are quoted dealing with the works begun in order to give better information about the irradiation conditions. Neutron fluence data have been so far reported as > 1 MeV values : with the present work a better correlation with the spectrum shape will be attempted taking into account the literature references. Magnetic and mechanical properties of specimens irradiated in different reactor positions will be tested : the irradiation facilities and the specimens set up are briefly described.
- c) Properties of some ASTM 212 type steels killed with Si, Al or Ti. New tests have been done to evaluate the transition temperature of these materials and a structure analysis has been also done in different heat treatment conditions.

CONTENTS

	Page
1. Introduction	1
2. Properties of iron alloys	3
2.1. Tensile tests	4
2.2. Impact tests	9
2.3. Fracture examination	16
2.4. Radiation damage investigation through changes in magnetic properties	23
2.4.1. Introduction	23
2.4.2. Specimens preparation	24
2.4.3. Magnetic measurements before irradiation	24
2.4.4. Specimens irradiation	24
2.4.5. Magnetic measurements after irradiation	25
2.5. Irradiation facilities set up and testing .	35
2.6. Set up of a furnace for recovery studies . .	35
3. Neutron spectrum influence on the radiation damage of iron	41
3.1. Outline to the problem approach	41
3.2. Specimens preparation for magnetic measure- ments	43
3.3. Specimen preparation for mechanical proper- ties	44
3.4. Irradiation facilities and preliminary tests	44
4. Mechanical properties of some modified ASTM A 212 steels	55
4.1. Impact properties	55
4.2. Microstructure	55
Bibliography	68

LIST OF FIGURES

- Fig. 2.1.1 - Grain size versus yield stress in FeTi alloys irradiated at different fluences and annealed
- Fig. 2.1.2 - Yield stress versus the cubic root of fluence in irradiated iron titanium alloys of different grain size
- Fig. 2.1.3 - Friction stress versus strain rate in iron titanium melt No. 54
- Fig. 2.1.4 - Yield stress versus strain rate in Ferrovac E tested at room temperature and at -78°C
- Fig. 2.2.1 - Impact energy versus test temperature in FeTi alloys irradiated at different fluences
- Fig. 2.2.2 - Impact energy versus test temperature in FeNiAl alloys irradiated at different fluences
- Fig. 2.2.3 - Impact energy versus test temperature in FeTi alloys irradiated at $2 \times 10^{18} \text{ n}(> 1 \text{ MeV}) \text{ cm}^{-2}$
- Fig. 2.2.4 - Impact energy versus test temperature in iron alloys irradiated and annealed at 300°C
- Fig. 2.2.5 - Impact energy versus test temperature in the FeTi alloy No. 57 irradiated and annealed at 300°C
- Fig. 2.3.1 - Twinned grains versus the distance from the notch in a FeNiSi impact specimen tested below the transition temperature (vertical section)
- Fig. 2.3.2 - Twinned grains versus the distance from the outer surface on the horizontal section of the same impact specimen as Fig. 2.3.1
- Fig. 2.3.3 - Twinned grains versus the distance from the notch in a FeTi impact specimen tested at liquid nitrogen temperature (vertical section)
- Fig. 2.3.4 - Surface of the fractured FeTi impact specimen (the same of Fig. 2.3.3) Unetched-400 x
- Fig. 2.3.5 - The same as Fig. 2.3.4 after nital etching-400 x
- Fig. 2.3.6 - Several aspects of the previous specimen. Unetched-400 x
- Fig. 2.3.7 - Several aspects of the previous specimen. Unetched-400 x

- Fig. 2.3.8 - The specimen of Fig. 2.3.4: area near the fracture(750 x)
- Fig. 2.3.9 - Electron microfractography of the specimen of Fig. 2.3.4 (5200 x)
- Fig. 2.3.10 - Section of the same specimen as Fig. 2.3.1 (750 x)
- Fig. 2.3.11 - Aspects of the previous specimen (1000 x)
- Fig. 2.3.12 - Aspects of the previous specimen (1000 x)
- Fig. 2.4.1 - Magnetization curve and hysteresis loop of sample T 295 A Fe Si 6.5% before annealing at 350°C. The shape of the loop shown in this figure is closely similar to the ones of samples T 295 B and C just before irradiation
- Fig. 2.4.2 - Magnetization curve and hysteresis loop of sample T 295 A after annealing at 350°C, before irradiation
- Fig. 2.4.3 - Magnetization curve and hysteresis loop of sample T 295 A after irradiation under a saturation field
- Fig. 2.4.4 - Typical viscosity field measurements as directly traced by hysteresigraph. The initial part only of each magnetization curve is of interest and therefore traced after the annealing periods shown to the right
- Fig. 2.4.5 - Magnetic viscosity field as a function of annealing time and annealing temperature for sample T 295 A
- Fig. 2.4.6 - Magnetic viscosity field as a function of annealing time and annealing temperature for sample T 295 B
- Fig. 2.4.7 - Typical recovery measurements. Viscosity field as a function of annealing time after demagnetization. Curve 1 is taken at the beginning of the recovery treatment at 142°C. Curves 2,3,4 are taken at later stages of the treatment. The fall of the field at a given time after demagnetization (100' in this figure) gives a measure of the recovery of the damage.
- Fig. 2.4.8 - Typical analysis of recovery measurements. The logarithm of the viscosity field measured 100' after demagnetization is reported as a function of total recovery time at given temperatures. The average slopes of these curves provide an estimate for the recovery time constant.

- Fig. 2.5.1 - Irradiation holder for tensile and impact test specimens
- Fig. 2.6.1 - Scheme of the annealing apparatus for damage recovery studies
- Fig. 2.6.2 - Annealing apparatus for damage recovery studies
- Fig. 2.6.3 - a) specimen heating rate-full line: Argon atmosphere-dotted line: in vacuo. b) specimen cooling rate
- Fig. 2.6.4 - Specimen heating behavior at different programmed heating rates of the furnace
- Fig. 3.1.1 - Mock up for activation monitors
- Fig. 3.2.1 - Aluminum holder for ultraperm sample irradiation
- Fig. 3.2.2 - Typical measurements before irradiation on ultraperm specimens
- 1) Hysteresis loop up to 0.8 Wb/m^2
 - 2) Same with enlarged field scale
- Fig. 3.2.3 - Typical measurements before irradiation on ultraperm specimens. Magnetization curve and hysteresis loop up to 0.5 Wb/m^2
- Fig. 3.2.4 - Typical measurements before irradiation on ultraperm specimens
- 1) Hysteresis Rayleigh type loop and initial permeability measurement
 - 2) Initial permeability measurement repeated with more sensible B scale
- Fig. 3.4.1 - Irradiation container for damage dosimetry experiments
- Fig. 3.4.2 - Irradiation container for damage dosimetry experiments
- Fig. 3.4.3 - Specimen holders for
- a) tensile tests (exploded view)
 - b) tensile tests (open)
 - c) ultraperm toroidal specimens
- Fig. 4.1.1 - Impact energy versus test temperature in aluminum killed ASTM A 212 steel
- Fig. 4.1.2 - Impact energy versus test temperature in silicon killed ASTM A 212 steel

- Fig. 4.1.3 - Impact energy versus test temperature in 0.3% titanium killed ASTM A 212 steel
- Fig. 4.1.4 - Impact energy versus test temperature in 1% titanium killed ASTM A 212 steel
- Fig. 4.2.1 - Hardness values on ASTM A 212 steels differently killed; treated for different times at 500, 600 and 700°C after austenitization at 850°C
- Fig. 4.2.2 - Summary of some structure aspects in steel specimens differently treated.

INFLUENCE OF NITROGEN IN IRON AND STEEL UNDER
FAST NEUTRON IRRADIATION ^(*)

1. Introduction

The present annual report deals with the work done in Sorin and in IENGF (Istituto Elettrotecnico Nazionale Galileo Ferraris - Torino) during the period October 1st, 1965 - September 31, 1966, under the contract N° 074-65-TEEI (RD).

During the past year, the research was partially devoted to bring to a conclusion the studies developed during the previous research contract (004-63-TEEI). At the same time a new series of complementary experiments has also been planned and begun, taking in account the results previously gathered. Part of the data and conclusions attained during the work have been reported, along the past year, in several papers appeared on specialized periodicals or presented in technical or scientific meetings. The titles of the papers, whose content will be, in some cases, briefly summarized in the present report with the aim of giving a better survey of the work done, have been previously quoted in the quarter reports 1, 2, 3. (**)

The general aim of the present research has been extensively described in several occasions and may be briefly summarized as the study of the influence of nitrogen on the neutron irradiated iron and steel; the problem was attacked during the first research contract, by comparing the mechanical properties and brittleness, before and after irradiation, of very low alloyed iron peculiarly characterized by the different interstitial elements distribution. By this means the possible interactions between impurities and defects have been evaluated and, meanwhile, the kind of defects affecting the magnetic properties of high purity iron have been studied through magnetic viscosity measurements of the material irradiated in and without magnetic field at temperatures below 50°C and following the changes in the magnetic viscosity itself through annealing (1).

Brittleness and mechanical properties of low iron alloys have been measured as a function of the grain size and of the neutron fluence; the results have been reported in (2), (3), (4).

The results obtained showed that, if the radiation hardening is evaluated as increase of the lower yield point ($\Delta \sigma_y$), the contributions due to source hardening (Δk_y) and to friction hardening ($\Delta \sigma_0$) put in evidence by the Cottrell (5)

(*) Manuscript received on January 17, 1967.
(**) SORIN Report M/440-441, 442

theory for the Petch (⁶) and Hall (⁷) equation

$$\sigma_y = \sigma_0 + k_y d^{-\frac{1}{2}}$$

should be considered dependent on ageing phenomena occurring in iron during irradiation. It was moreover observed that in the interstitial free iron the Petch relationship can be considered a too simple interpretation of yielding, which does not take into account the contribution due to the obstacles opposing the dislocations movement within a single grain. In any case the Petch analysis appeared to be still useful to put in evidence, in the non irradiated alloys, a different strain rate effect dependent on the impurity distribution and, in the irradiated materials, a different radiation hardening and recovery behavior.

Impact tests showed different transition temperatures in iron alloys, depending on the nitrogen distribution, and free nitrogen, together with the different killing elements, appeared to be very important in increasing the transition temperature during irradiation (³) (⁸). Impact tests are now reported in which the transition temperature is measured on specimen irradiated at increasing fluences: the specimens were prepared from iron alloys containing aluminum or titanium in small concentration and, while tensile tests on the same materials gave different results, impact responses are practically identical.

As a consequence, either due to the difficulty of clarifying only by means of the Petch relationship the radiation damage mechanism, or due to the necessity of better correlating the impact and tensile properties of the materials in test, it seemed convenient to enhance the research interests to the study of the strain rate and temperature effect on the mechanical properties of iron either in presence of free interstitial atoms or after their complete precipitation. By this way it should be possible to obtain, through the activation volume for yielding, some indications about the kind of obstacles which affect the dislocations movement in irradiated bcc metals.

It appeared, moreover, that a better knowledge of the nitrogen distribution in iron alloys and of its precipitation kinetics in presence of different killing elements after decomposition, by quenching, of the precipitated nitrides, might give some contribution to clarify the mechanical properties of irradiated iron and steel; a study about the subject is now begun on suitably prepared steel melts of ASTM A 212 base composition, added with different killing elements (Al, Si, Ti), whose microstructure and metallurgical properties are briefly detailed in the present report.

At the same time it seemed interesting to continue the investigation on the nature of defects introduced by irradiation through changes of magnetic properties. The previous magnetic viscosity experiments, performed at the IENGF (1), had shown that in pure iron after irradiation at about 50°C the formed defects, responsible for magnetic viscosity, were likely to be vacancies bound to impurities. These defects were mobile from about 60°C and precipitated between 120 and 250°C. They might actually also contribute to the changes in mechanical properties which were observed in recovery experiments between 100 and 200°C.

In the new group of experiments, performed on magnetic properties of irradiated samples, specimens of iron with an high silicon content were irradiated and the magnetic viscosity and recovery of the effects was studied to get information, in general, on the effect of alloying elements on the mobility and density of defects. The examination of silicon iron 6,5% seemed also of interest since this alloy is characterized by a zero magnetostriction. If the irradiation effects on magnetic properties were in some way related to internal strains, the radiation damage on magnetic properties in this alloy should appear strongly reduced.

Finally the research has been extended to the study of the neutron spectrum effect on the radiation induced defects distribution. The research was principally planned in order to give a better significance to the dose evaluation data, so far reported as > 1 MeV; it is moreover known that in some alloys of the permalloy type, strong changes in permeability are observed in the course of irradiation and the effect is related to the number of displaced atoms. Since the effect can be measured very easily, it seems of interest to correlate this damage effect with the changes of mechanical properties observed in iron specimens irradiated in different neutron spectrum shapes.

2. Properties of iron alloys

In the present chapter are summarized the results obtained with tensile and impact tests on iron alloys whose preparation and composition have been previously reported (see point II.1 and table II.1 in (1)); further sections are devoted to the description of the irradiation and annealing devices and in two other sections will be reported the results obtained

by measuring the magnetic properties of irradiated Fe-Si and during some structural examination of fracture surfaces.

2.1 Tensile tests. (by M. Castagna)

a) A new set of post-irradiation tests has been done on two Fe-Ti alloys (n° 57 and 52) containing a large titanium concentration respectively irradiated at the fluences of 0.7 and $3 \times 10^{18} \text{n} (> 1 \text{ MeV}) \text{ cm}^{-2}$. The figure 2.1. shows the correlation 0.2% proof stress versus grain size obtained on these materials in comparison with other Fe-Ti alloys irradiated at higher fluences, already quoted in (3). It is evident that in the coarse grain size region the Hall-Petch relationship does not seem to be well followed; in fact, while the lowest exposure levels cause a slight lowering in the k_y value according to the results of other Authors for iron (9) and molybdenum (10), a saturation effect of the damage, as measured by the increase of yield strength, is observed for fluences above $1 \times 10^{19} \text{n cm}^{-2}$. The effect of the fluence on the yield stress σ_y for three grain sizes is summarized in figure 2.1.2; over the whole irradiation range the increase of σ_y is well described by a $(\phi)^{1/3}$ variation for the fine and medium grain size, while the mentioned saturation effect in the coarse grain size region is evident.

Annealing treatments have been continued up to 350°C on tensile specimens from the melts n° 40,48 and 56 irradiated at $1.10^{19} \text{n cm}^{-2}$. Some preliminary results were reported in (3) (4). In table 2.1 the percent recovery of yield stress in various post irradiation annealings for the different materials are summarized.

b) A new approach to the study of deformation both in irradiated or unirradiated bcc metals has been recently attempted by some Authors (11) on the basis of a detailed theory (12) (13) (14) for the strain rate and temperature dependence of yield strength. As some difficulties have been found using the grain size analysis to study the irradiation hardening, this way seems to be useful to gain some more information on the radiation effects.

The influence of strain rate ($\dot{\epsilon}$) on yield stress has been checked at room temperature in the range of 3×10^{-4} to $1 \times 10^{-2} \text{ sec}^{-1}$ on a unirradiated Fe-Ti specimens (melt n° 54): in figure 2.1.3. the friction stress σ_0 is plotted versus $\log \dot{\epsilon}$. Measurements of the strain rate dependence of the yield stress have also been done on Ferrovac E specimens at room temperature and at -80°C in the range 6.5×10^{-5} to $4.5 \times 10^{-2} \text{ sec}^{-1}$ (Part of the results are reported in fig. 2.1.4, in which each point is

the average of at least two results.

Measurements at -190°C and in a wider and better distributed range of strain rates are now in progress.

TABLE 2.1 - Percent recovery of yield stress in post-irradiation annealing of different materials (three grain sizes)

Material	Annealing treatment								
	6 h 130°C	28 h 130°C	192 h 130°C	6 h 200°C	28 h 200°C	96 h 200°C	6 h 300°C	96 h 300°C	96 h 350°C
c.g.	-	-	0	12	23.5	36.5	-	-	-
40m.g.	-	-	0	0	0	21.6	-	-	-
f.g.	-	-	0	-16	-6	0	-	-	-
c.g.	-	-	~6.5	-	-	25	-	49	62
48m.g.	-	-	~8	-	-	25	-	46.5	61
f.g.	-	-	0	-	-	25	-	52.5	63
c.g.	0	-	0	-8	-	-	55	-	-
56m.g.	0	-	0	2.5	-	-	55	-	-
f.g.	0	-	0	10	-	-	68	-	-
c.g.	-	-2.3	-	-	-3.25	-	-	-	-
29m.g.	-	1.6	-	-	8	-	-	-	-
f.g.	-	4.4	-	-	12	-	-	-	-

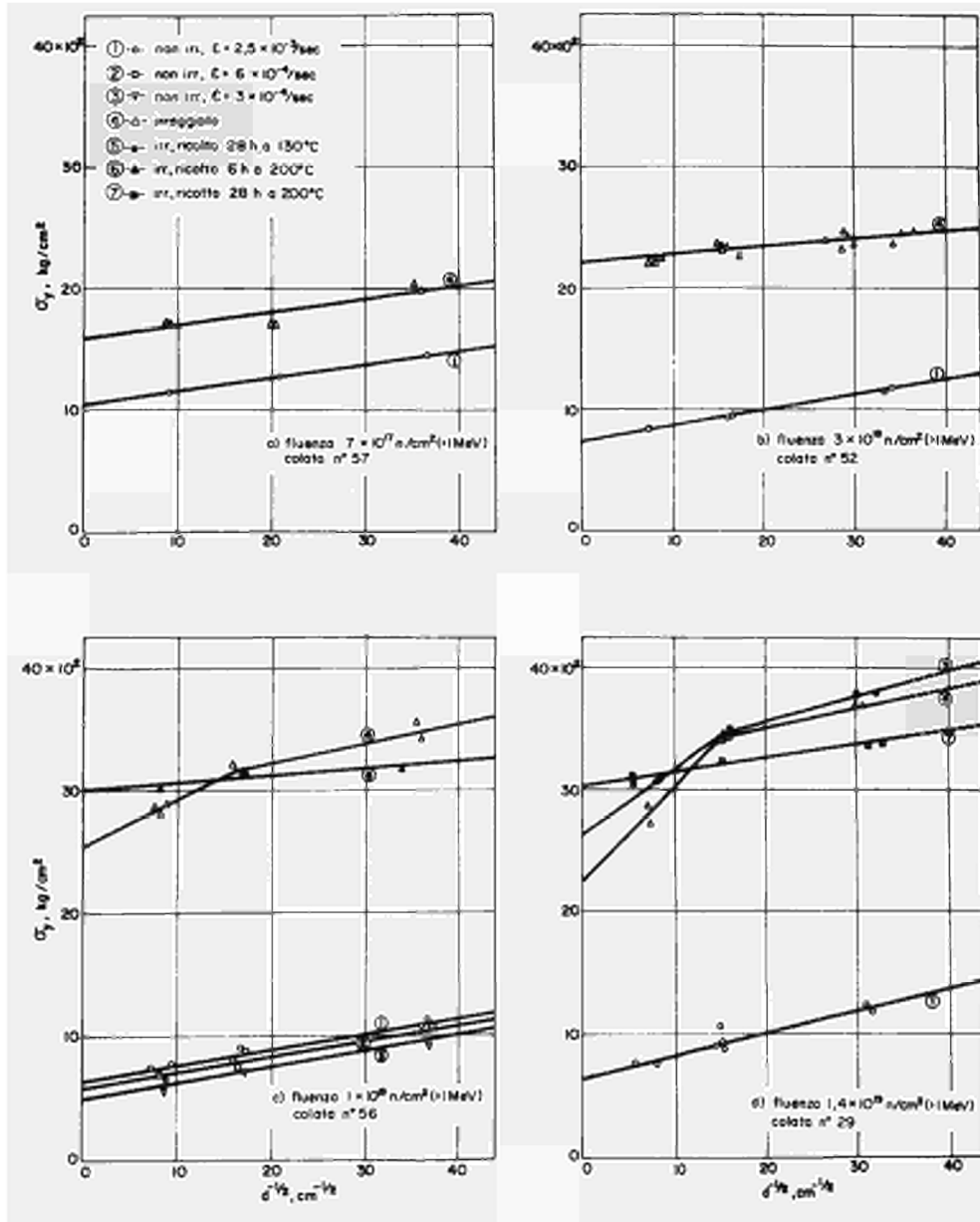


Fig. 2.1.1

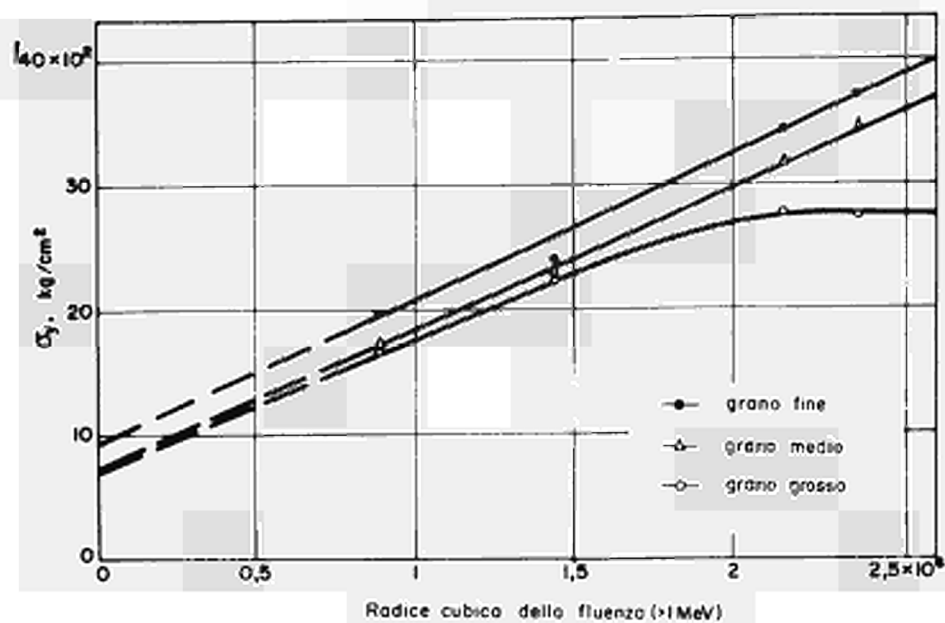


Fig. 2.1.2

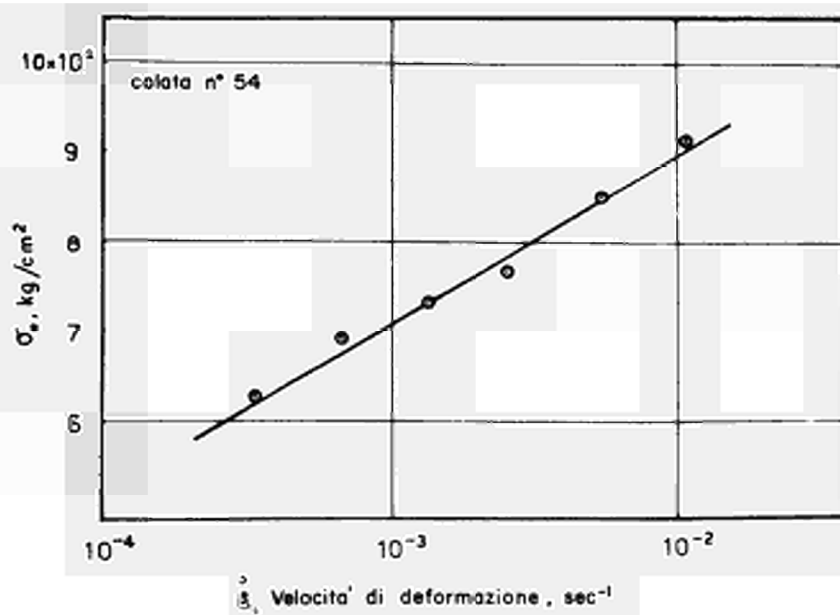


Fig. 2.1.3

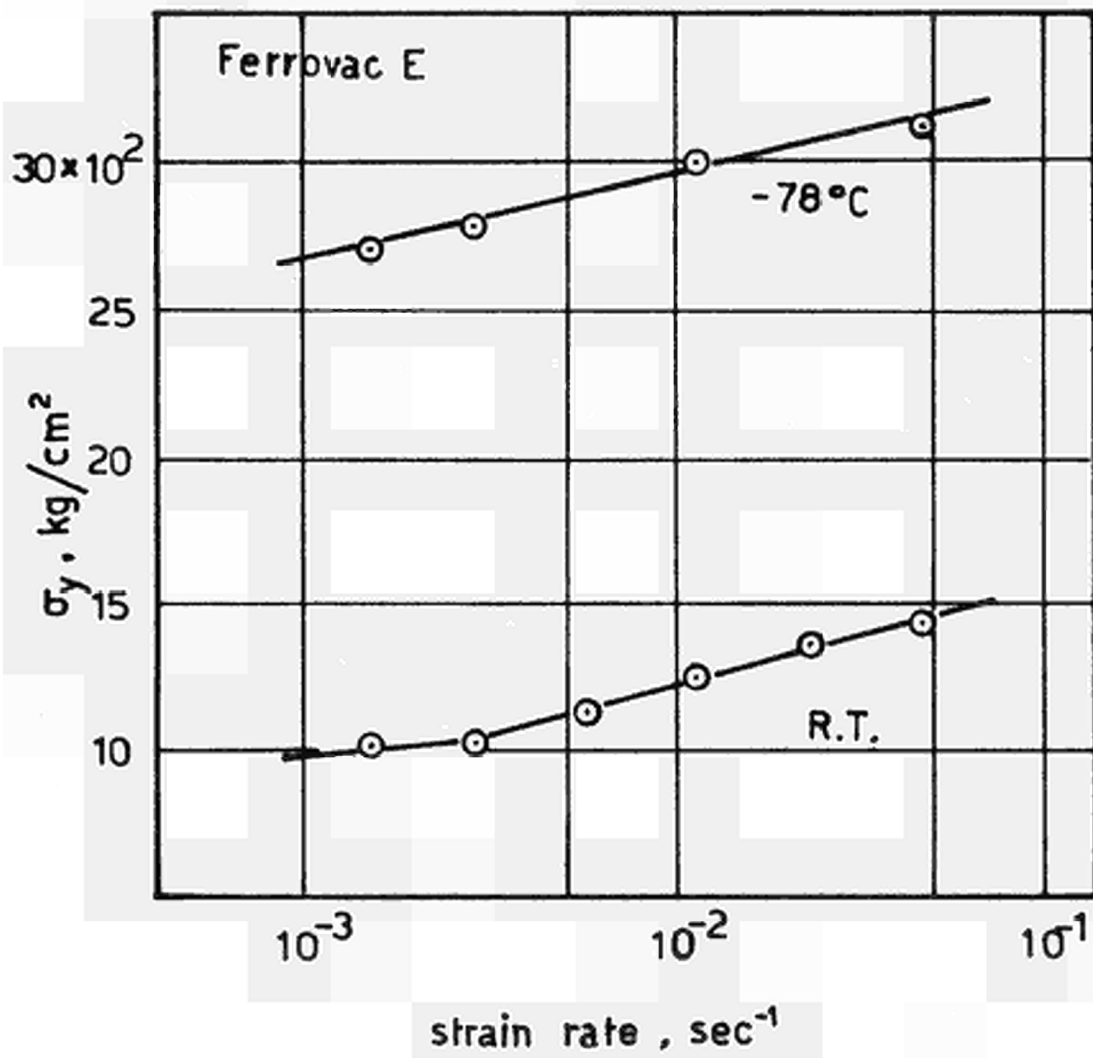


Fig. 2.1.4

2.2. Impact tests (by F.S. Rossi and A.A. Rossi)

As a continuation of the tests done during the first research period (1), the ΔTT (transition temperature increase) has been measured on several iron alloys irradiated at increasing fluences from 0,5 to $10 \times 10^{18} \text{n} (> 1 \text{ MeV}) \text{ cm}^{-2}$. In particular the tests have been done on Fe-Ti and Fe-N-Al alloys; their transition curves are respectively reported in figures 2.2.1. and 2.2.2.

In general, it may be observed that at the lowest fluences ΔTT is practically zero and that the full ductility plateau (specially in Fe-N-Al alloys irradiated up to 2×10^{18}) is generally markedly lowered, also if a sudden peak is evident immediately above the transition.

In the Fe-Ti alloys it seems that up to fluences of 2×10^{18} the ΔTT remains very small, while at fluences of 1×10^{19} it is practically identical to that of Fe-N-Al. In figure 2.2.3. are reported the transition curves of two Fe-Ti alloys: both materials have an actual composition in which titanium may be considered insufficient (melt n° 28) or just sufficient to give the complete interstitials precipitation (melt n° 26). The grain size analysis gave for the first of them a k_y value high enough to justify the interstitials locking effect on dislocations while for the second one the k_y value appeared to be very small. Both materials showed, after irradiation at the same fluence of $2 \times 10^{18} \text{n cm}^{-2}$, a ΔTT value similar to that observed in Fe-N-Al irradiated at the same fluence, while the Fe-Ti alloy n° 52 (containing Ti in large excess) shows in the same conditions a smaller ΔTT .

Another set of tests has been developed to check if the secondary embrittlement observed in some steel specimens irradiated and submitted to very long annealing cycles at 300°C should be ascribed, in agreement with some authors, to ageing phenomena or could be considered independent from the presence of interstitials in the iron matrix. Three iron alloys (Fe-N-Al n° 46, Fe-Ti n° 56 and 57) irradiated at $1 \times 10^{19} \text{n cm}^{-2}$ have been annealed at 300°C for times up to 300 h and the ΔTT was measured. The results are reported in figure 2.2.4.

The recovery rate seems to be slower in the presence of interstitials: a treatment of 200 h or only of 50 h seems to be sufficient to restore the transition temperature to the original (non irradiated material) values in the melts n° 56 and 57 but not in the melt n° 46; it is however to be emphasized that secondary embrittlement has been observed

either in Fe-Ti or in Fe-N-Al alloys after a treatment of 300 h, the fact bringing to the conclusion that the secondary brittleness is independent of ageing phenomena.

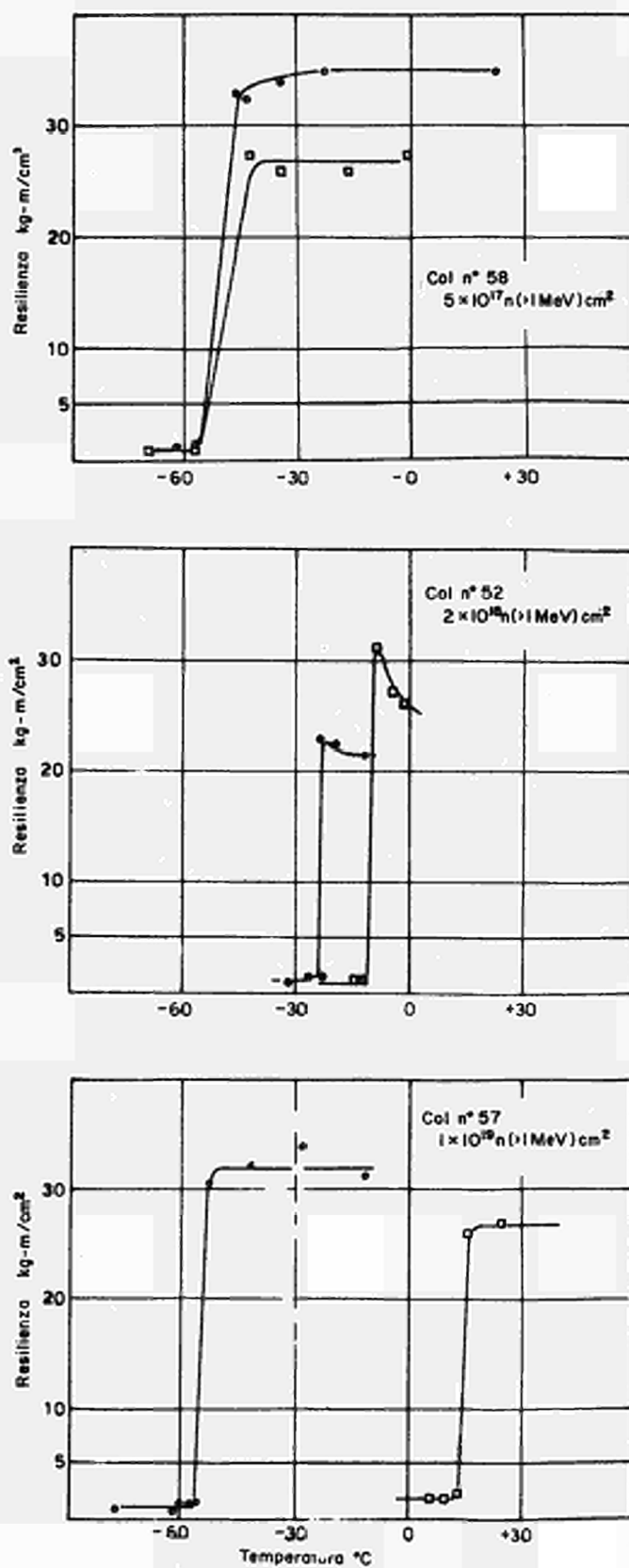


Fig. 2.2.1

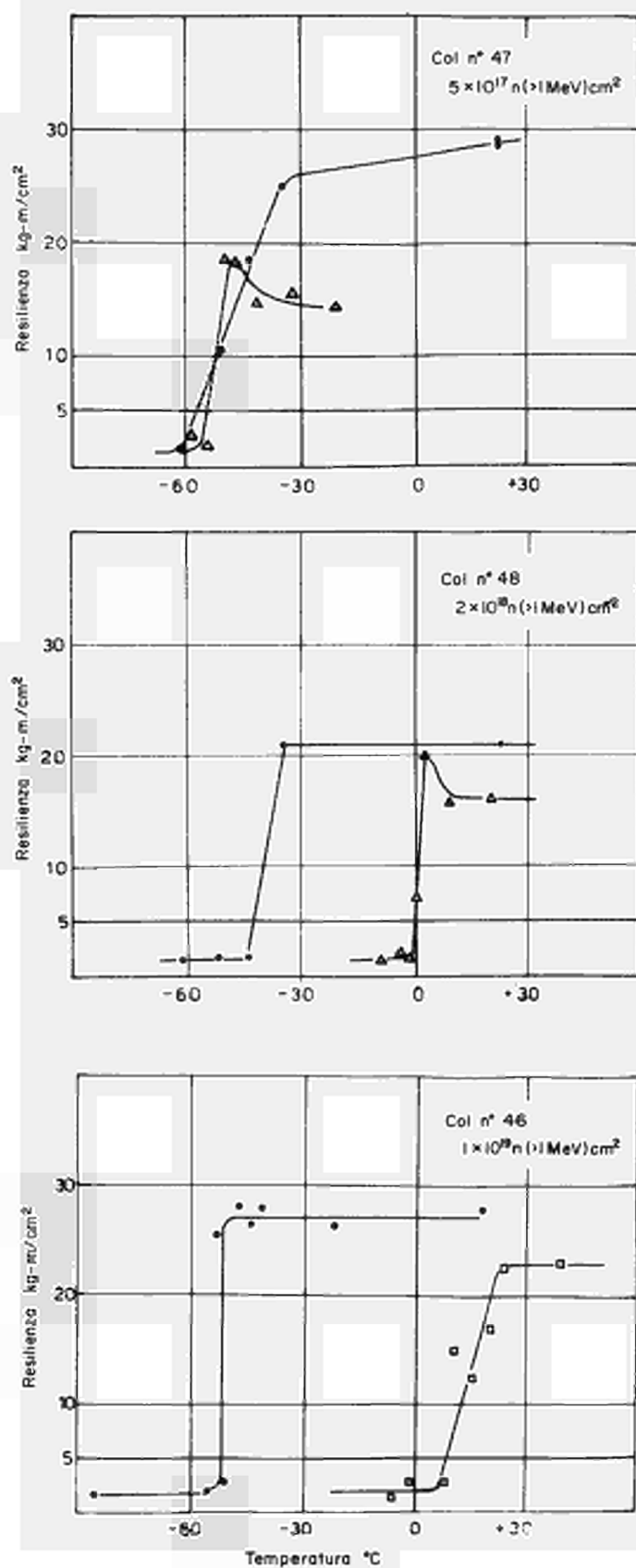


Fig. 2.2.2

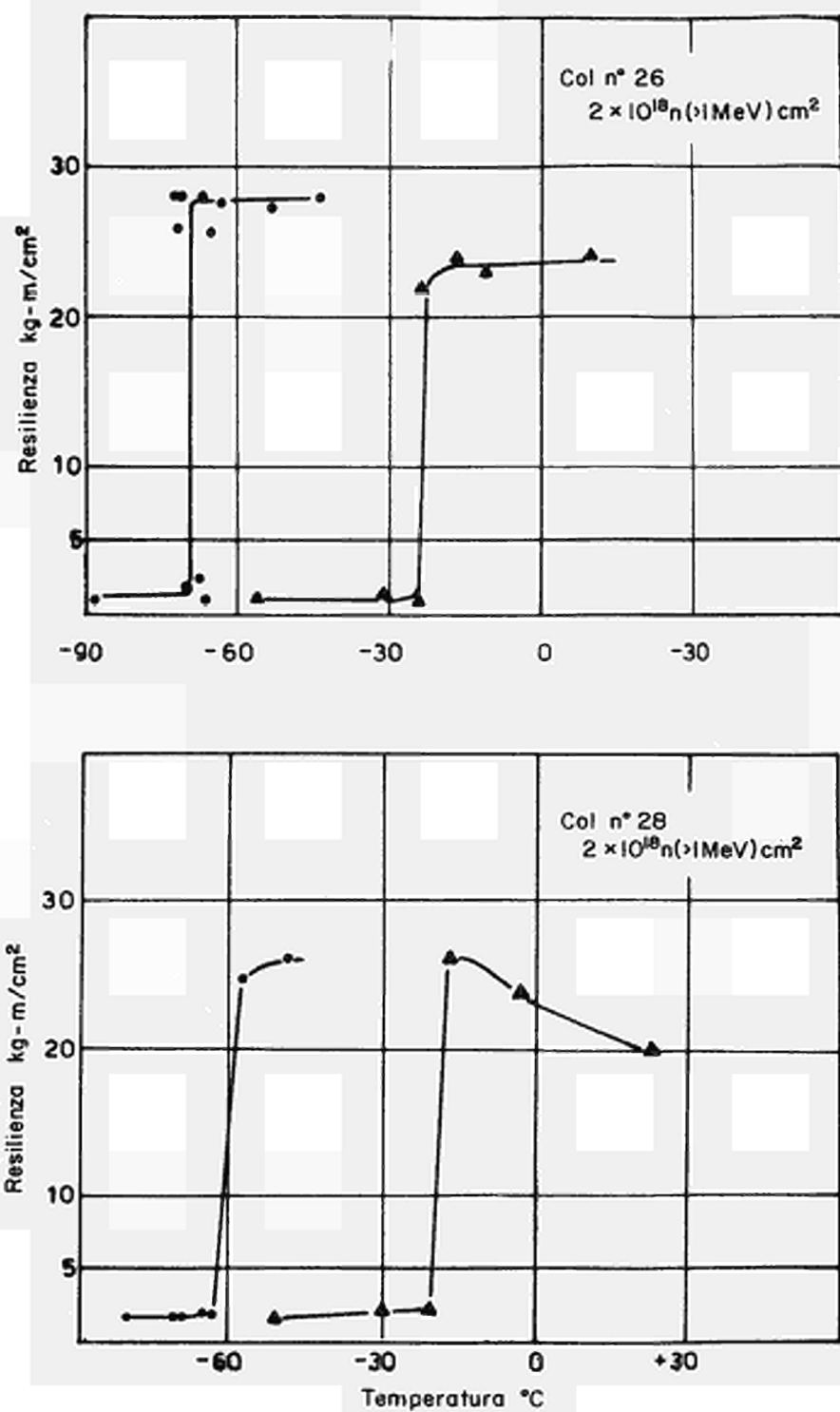


Fig. 2.2.3

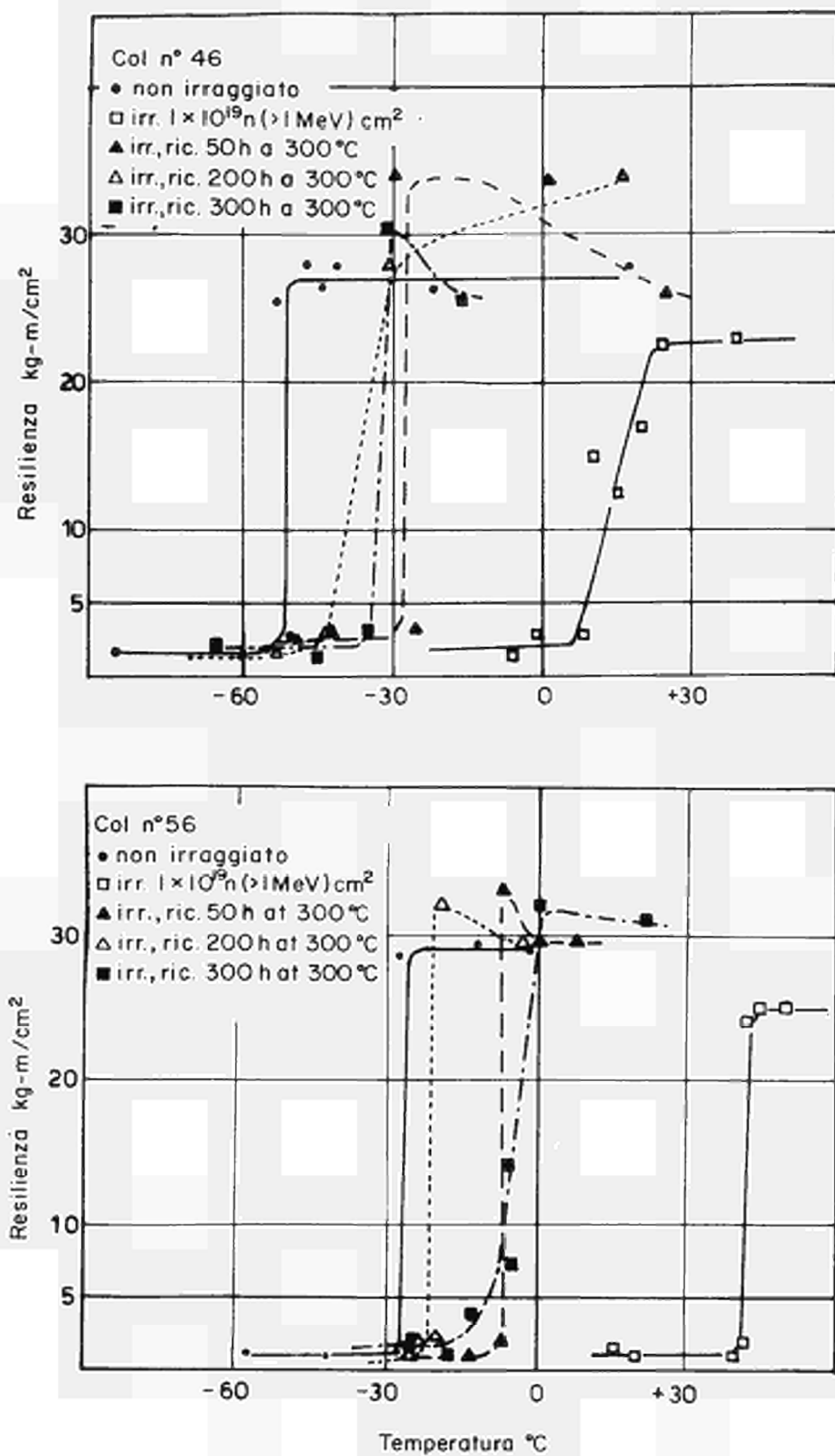


Fig. 2.2.4

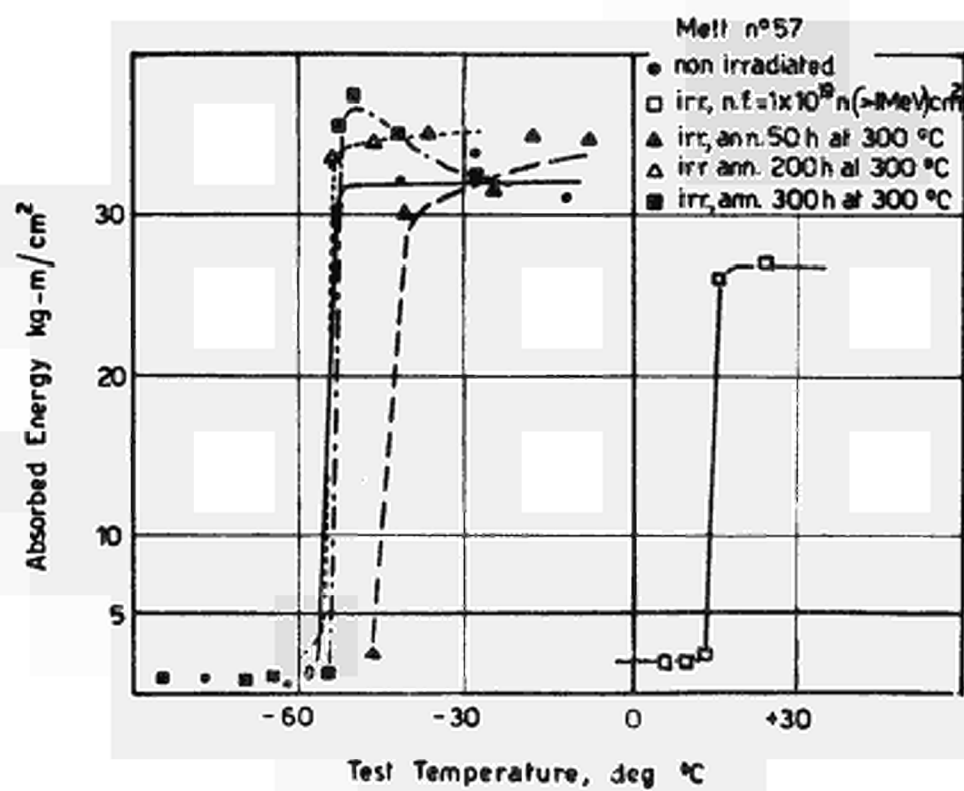


Fig. 2.2.5

2.3 Fracture examination (by F.S. Rossi and M. Rossi)

As a first approach to the study of the influence of impurities on the grain size sensitivity of the transition temperature of iron (20) some metallographic examinations have been done on Fe-N-Si and Fe-Ti alloys, with the aim of evaluating the twin distribution and the temperature of their appearance on the fracture surface.

The twin concentration measured on two orthogonal sections both normal to the fracture surface has been plotted in figure 2.3.1. versus the distance from the notch and in figure 2.3.2. versus the distance from the external surface of a Fe-N-Si the specimen broken below the transition; in both figures the data refer to sections cut at different depth. The twin concentration is expressed as the twinned grains number per examined area (1 mm^2) and it appears that the larger twin concentration corresponds to the central zone of the surface area at a certain distance from the notch root.

Measurements of the twin distribution in a Fe-Ti specimen are reported in Figure 2.3.3.; the specimen was broken at the liquid nitrogen temperature and the twins appeared to be present in larger number along an external zone of the fracture surface and at a distance of several mm from the notch root. In figures 2.3.4. and 2.3.5. and 2.3.6., 2.3.7. are shown some aspects of the specimen near the fracture before and after etching of the surface. Figure 2.3.8. shows a frequent aspect of twin distribution in a zone near the fracture, 1 mm from the external surface of the specimen.

Intergranular cracks were never observed on Fe-Ti specimens by optical examinations, while they appeared in some unfrequent cases when the fracture surface replica is observed by electronic microscope* (see figure 2.3.9.); in the Fe-N-Si specimens, twinning is frequently joined with intergranular cracks. (See fig. 2.3.10) and this kind of fracture was observed either by electron or optical microscope. In this material twins were frequently observed to originate from inclusions (see fig. 2.3.11, 2.3.12).

(*) Electron microfractographies have been kindly done by Dr. Mojoni (IENGF) who is here acknowledged.

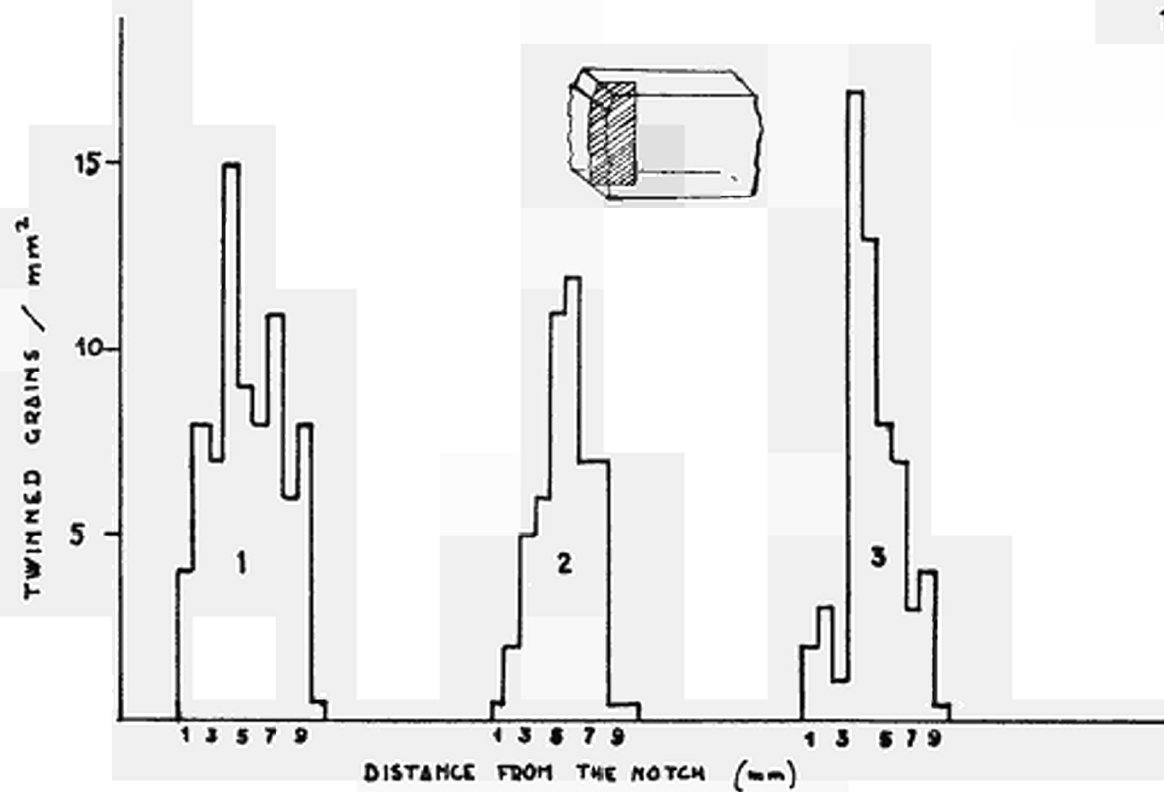


Fig. 2.3.1

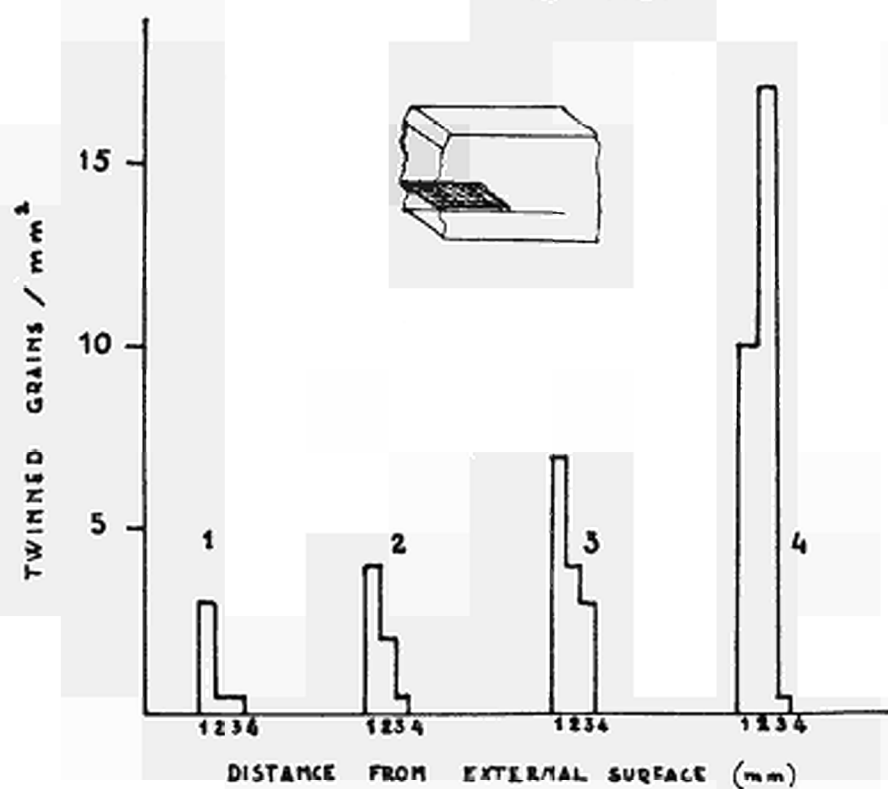


Fig. 2.3.2

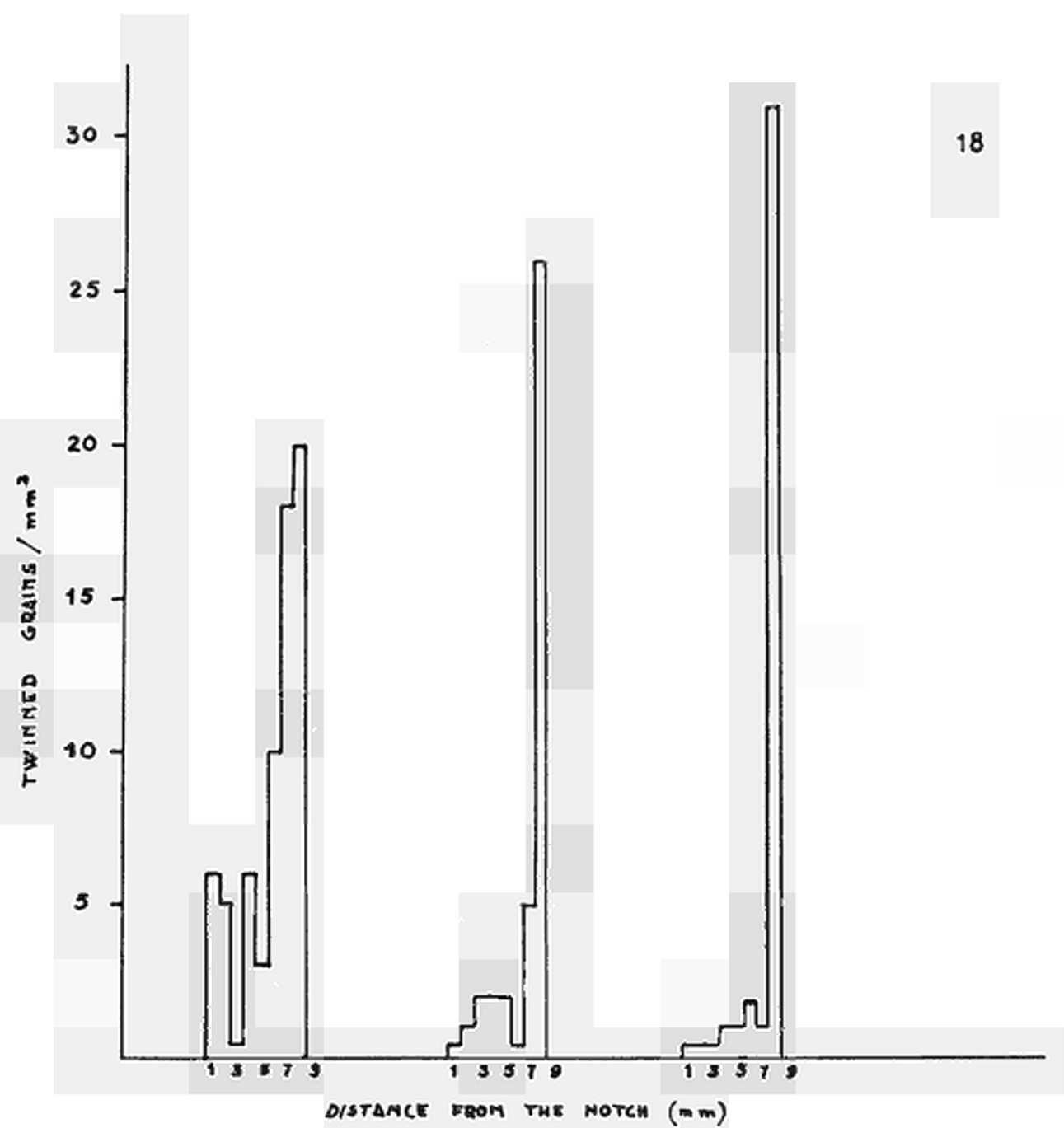


Fig. 2.3.3

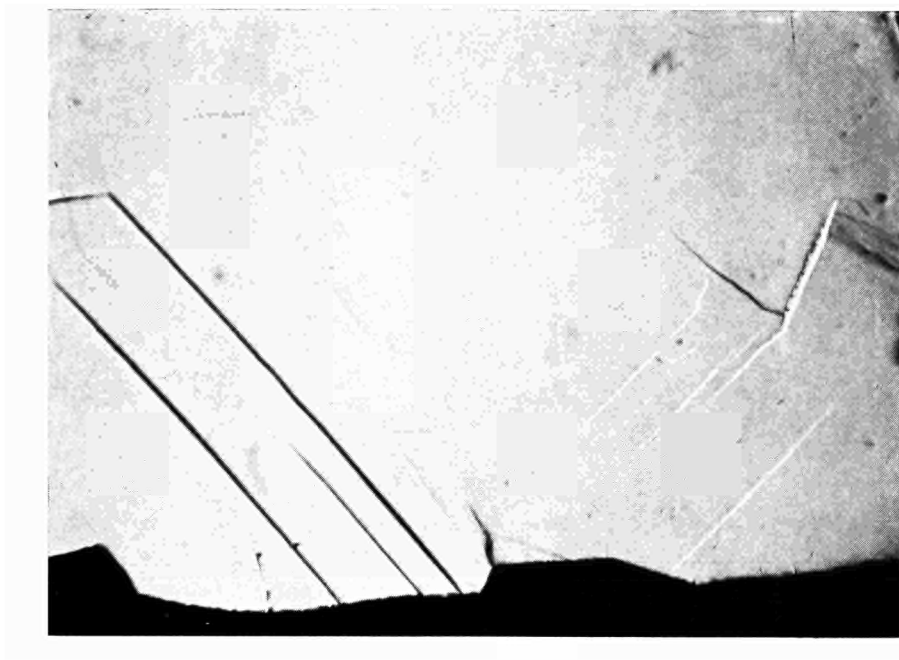


Fig. 2.3.4

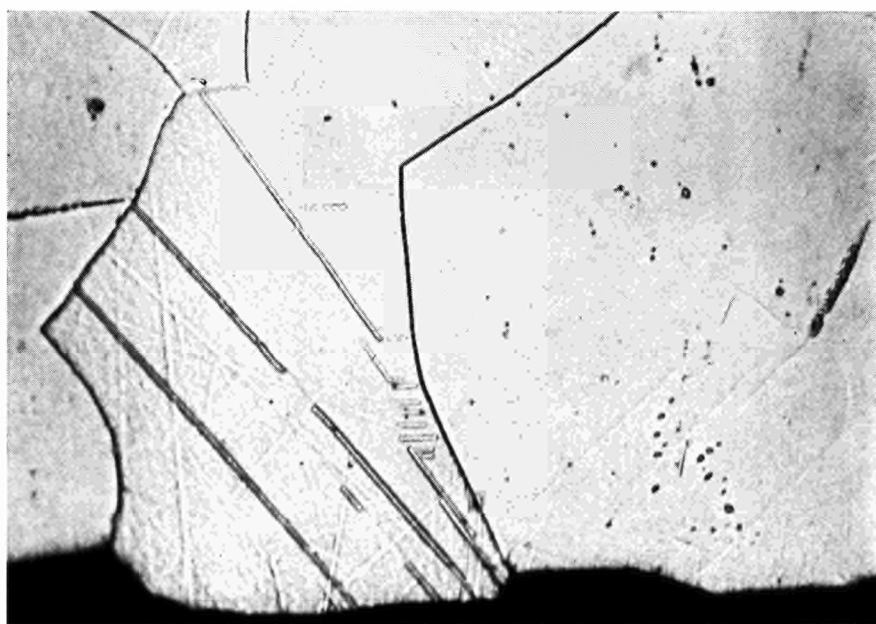


Fig. 2.3.5

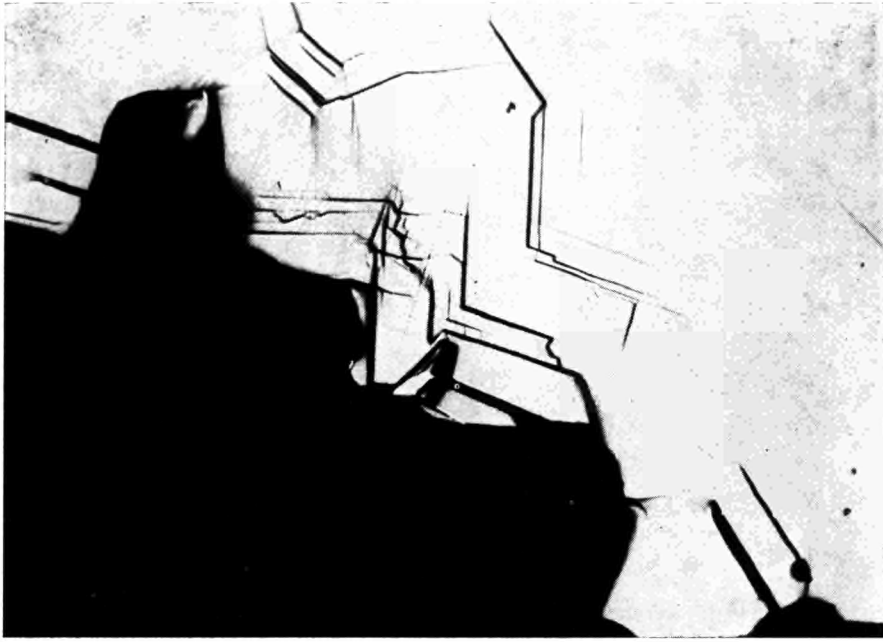


Fig. 2.3.6



Fig. 2.3.7

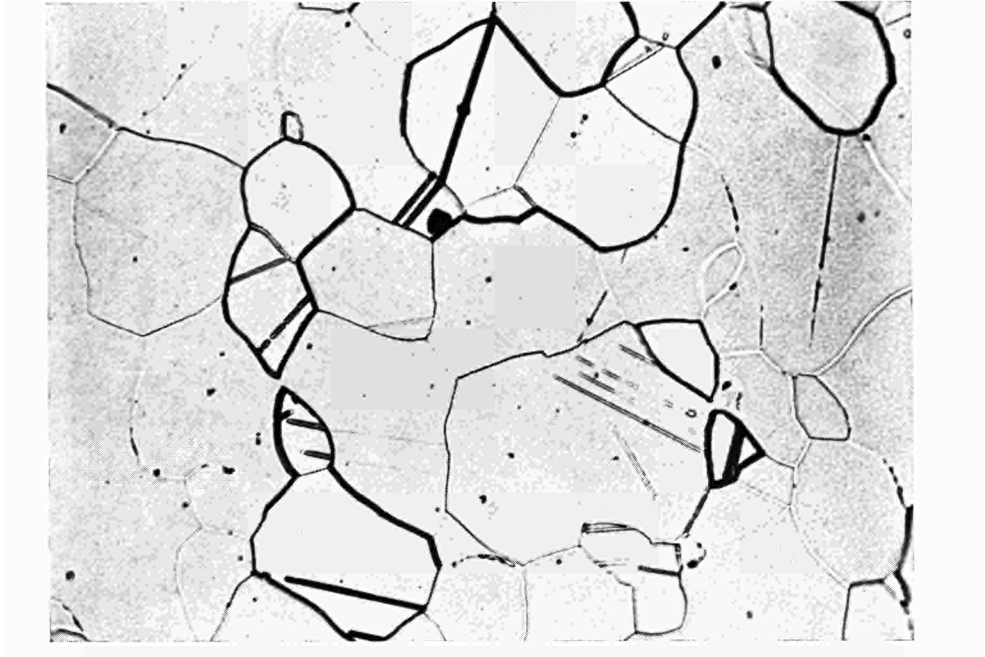


Fig. 2.3.8

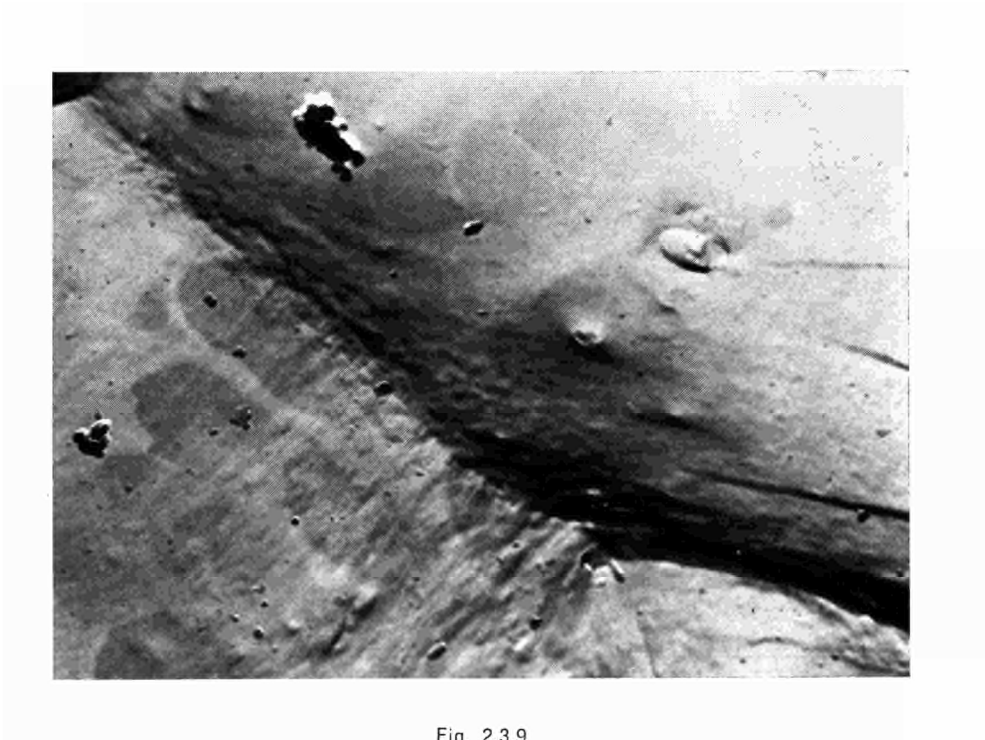


Fig. 2.3.9

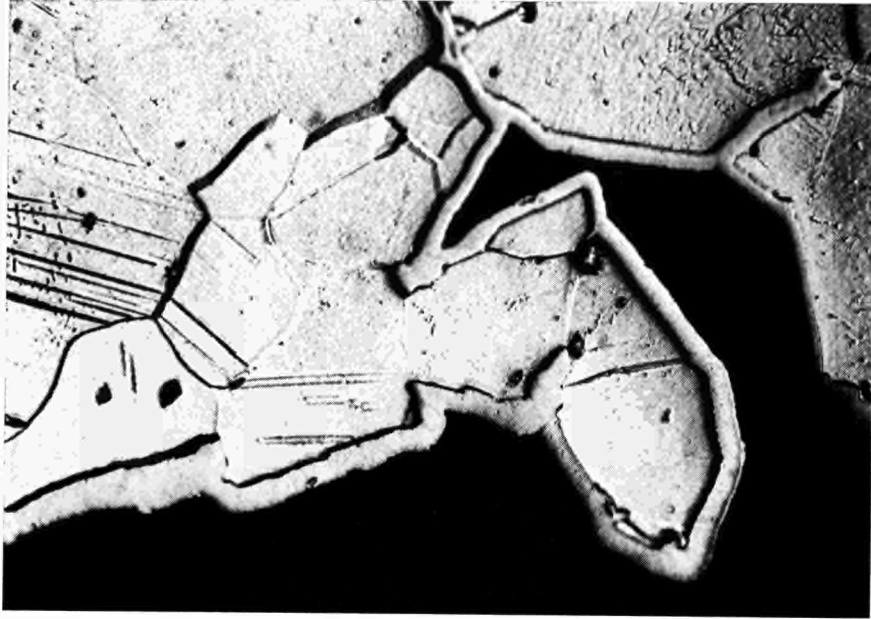


Fig. 2.3.10

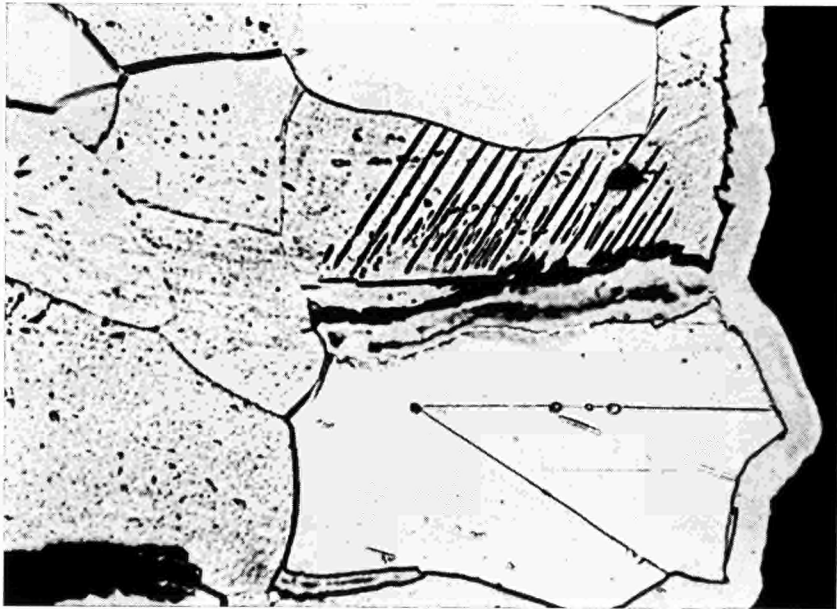


Fig. 2.3.11

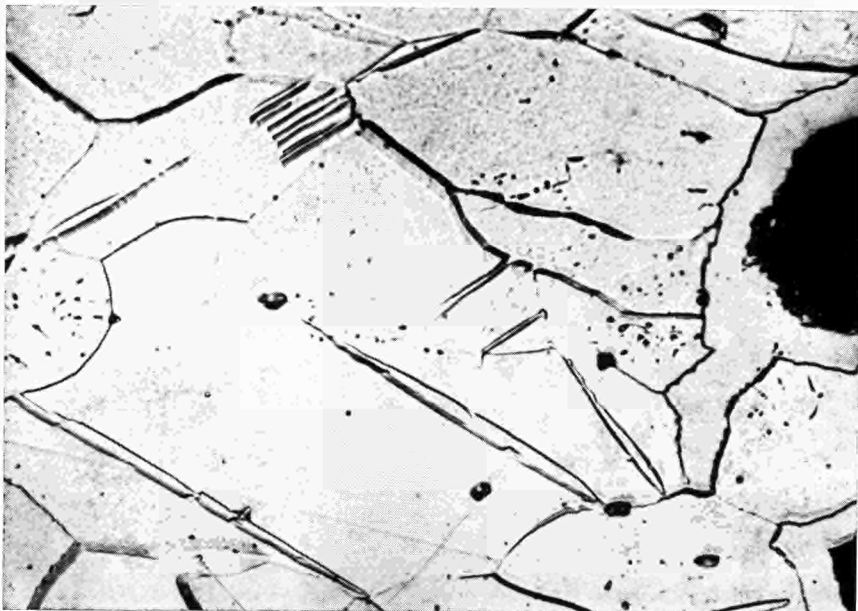


Fig. 2.3.12

2.4 Radiation damage investigation through changes in magnetic properties (by A. Ferro, G. Montalenti, G.P. Soardo (IENGF))

2.4.1. - Introduction.

In the preceding research period ⁽¹⁾ the study of magnetic viscosity effect due to neutron irradiation in pure iron had shown that at least a part of the defects introduced around room temperature is likely formed by vacancies associated to impurities or by divacancies, or in any case by very mobile defects with some uniaxial magnetic anisotropy. These defects are in fact mobile already around 50°C (the irradiation temperature) with a diffusion activation energy of about 0.85 eV. Annihilation of these defects occurs between 100°C and 200°C on sinks characterized by an average distance of the order of 10^{-5} cm, as obtained from the recovery kinetics.

These results were recently presented at the Cairo Solid State Conference, Interaction of Radiation with Matter, September 1966 ⁽¹⁵⁾.

In the research period which concerns this report, a similar investigation was performed on 6.5% silicon iron alloy. The reasons for this investigation are the following:

- a) The comparison of the diffusion and annihilation kinetics of the irradiation defects in the pure and strongly Si-doped iron may show whether these kinetics are dependent or not on the presence of alloying elements.
- b) The use of Si as alloying element still permits to obtain specimens characterized by very high permeability values, of the same order as in the pure Cioffi iron employed in the former investigation, thus making the comparison of the irradiation effects significant.
- c) A Fe-Si alloy with 6.5% Si is characterized by an almost zero magnetostriction ⁽¹⁶⁾, therefore magnetic viscosity effects measured after irradiation are insensitive to large size defects, which may act as internal strain sources, and a comparison with pure iron results should permit to further establish the nature of defects responsible for magnetic properties variations.

In the present report a detailed description is given of preparation of samples, irradiation, and magnetic measurements before and after irradiation. Since these measurements have not yet been completed on all samples, a general discussion on the results will be given in a future report.

2.4.2. Specimens preparation.

Specimens had already been prepared during the preceding research period. No preparation details had, however, been given in former technical reports. Preliminary preparation tests were made on a Fe-Si 3.5% alloy. Maximum permeability values obtained were, however, poor. Because of the low magnetostriction value of the Fe-Si 6.5% composition, much higher permeability values can be expected. Because of the high brittleness of this alloy it is, however, difficult to machine the ingots into toroidal specimens. Therefore hollow ingots were directly prepared in order to obtain the finished samples by grinding technique only. The alloy was melted in a resistance furnace in hydrogen atmosphere. Solidification of ingots was obtained in vacuum to avoid blowholes. After machining the specimens (toroids with o.d. 35 mm; i.d. 28 mm, thickness 7 mm), these were annealed in pure dry hydrogen for 24 hours at a temperature close to the melting temperature, and slowly cooled down. Starting from about 700°C a saturation magnetic field was applied to the samples. Maximum permeability after this magnetic annealing is of the order of 360,000. Before magnetic annealing μ_{\max} is only of the order of 50,000. Six similar samples were prepared. Two of them has to be discarded since their magnetic characteristics clearly showed the presence of small air gaps, which strongly reduced the specimens permeability. Four samples were packed in suitable aluminium containers with the measuring windings.

2.4.3. Magnetic measurements before irradiation.

On all samples the magnetization curve and hysteresis loop were recorded by means of an electronic magnetic curve tracer (17). Typical result are shown in Fig. 2.4.1. Detailed measurements of magnetic viscosity effects possibly present before irradiation were taken, through annealing stages after demagnetization up to 350°C, on one of the samples (T 295 A). These measurements did not show any appreciable viscosity up to about 350°C, where the viscosity effects due to Si couples becomes evident (18). Since these annealing treatments were performed in the demagnetized condition, a partial destruction occurred of the directional order of the Si couples obtained during the sample preparation by magnetic annealing. As a result a reduction in loop squareness appeared as shown in Fig. 2.4.2, compared to Fig. 2.4.1.

2.4.4. Specimens irradiation.

The four specimens were irradiated with an average fluence of 3×10^{17} thermal neutrons cm^{-2} , and 10^{18} fast neutrons

(>1 MeV) cm^{-2} at a temperature of about 52°C , in the Avogadro swimming pool reactor of SORIN, Saluggia. Three specimens were irradiated under a saturation magnetic field, and one in an apparently demagnetized condition. After a period of activity decay of about one month, magnetic measurements were taken on the irradiated samples.

2.4.5. Magnetic measurements after irradiation.

a) Magnetic curve and hysteresis loop.

The magnetization curve and hysteresis loop were measured after irradiation. The following results are obtained:

- I - Sample T 295 A: Irradiated under magnetic field. Hysteresis loop before irradiation shown in Fig. 2.4.2. After irradiation the hysteresis loop is modified with respect to Fig. 2.4.2. and assumes the slightly more square shape shown in Fig. 2.4.3.
- II - Sample T 295 B: Irradiated under magnetic field. Shape of the loop before irradiation similar to the one shown in Fig. 2.4.1. After irradiation no significant change in the loop shape is observed.
- III - Sample T 295 C: Irradiated under apparently demagnetized condition. Shape of the loop before irradiation is identical to the one shown in Fig. 2.4.1. After irradiation no significant change in the loop shape is observed.
- IV) - Sample T 296 A: Irradiated under magnetic field. Shape of loop before irradiation showed some instabilities. After irradiation the magnetization curve showed clear presence of small air gaps, which were probably present to a lesser extent before irradiation, and were enhanced by handling or by contact with the swimming pool reactor water. This sample was therefore discarded.

We briefly notice here that the behavior of sample I) shows that the effect of irradiation under magnetic field is similar to a magnetic annealing. The squareness increase may be attributed either to an increase of order of the Si couples enhanced by the irradiation through vacancies formation, or to the formation of anisotropic defects as in the case of pure iron. The behavior of sample II) is consistent with either explanation, while sample III) should be expected to show a squareness reduction after irradiation, which, however, is not observed. It is possible that sample III) was irradiated in a state of non zero magnetization and thus close to the magnetic state of sample II).

b) Magnetic viscosity measurements

Magnetic viscosity is measured by comparing the magnetization curve traced immediately after demagnetization with curves traced after increasing annealing times after demagnetization. All curves are traced by means of the automatic hysteresigraph. Curves after annealing show an initial almost straight part, which corresponds to the viscosity field, as shown in Fig. 2.4.4., which is a record of some measurements as directly traced by the hysteresigraph. Each trace corresponds to the time of annealing at 70°C after demagnetization, shown to the right. Only the initial parts of the magnetization curves are of interest and therefore traced. Measurements are taken at increasing times following demagnetization up to 24 hours, during isothermal treatments from about 40°C up to 90°C in steps of 10°C. The annealing temperature is stabilized within ± 0.2 °C. Recovery effects are observed between 90°C and 300°C.

In Figs. 2.4.5. and 2.4.6. viscosity field values measured on samples T 295 A and T 295 B are reported as a function of annealing time after demagnetization. In Fig. 2.4.6. the systematic dispersion of the experimental points does not seem to be related to errors, and suggests that the points be joined by the curves shown. A correction may possibly result from careful measurements on sample T 295 C, yet to be examined.

Recovery data on the same samples are obtained at higher temperatures (between 90 and 300°C) as follows. The viscosity field as a function of annealing time after demagnetization is measured at the beginning of any given recovery stage (curve 1 in Fig. 2.4.7.). The same measurements are repeated after convenient recovery periods (curves 2,3,4 in Fig. 2.4.7.). The decrease of the viscosity field value at a given time after demagnetization, say 100' as in Fig. 2.4.7, as a function of total recovery time, is a measure of the recovery of the magnetic damage. In Fig. 2.4.8 this decrease is shown as a function of total annealing time: this time is plotted on the horizontal axis, while on the vertical axis the viscosity field values measured 100' after demagnetization are reported. From the average slopes of the curves of Fig. 2.4.8 one obtains for the recovery time constant an estimated value of the order of 100 hours around 150-200°C. Unfortunately the data relative to samples T 295 A and T 295 B are rather dispersed (only a few results are actually shown in Figs. 2.4.7. and 2.4.8.) and do not allow clear estimates of these time constants.

These data will be analyzed and discussed in a future report when the data relative to all specimens will be available.

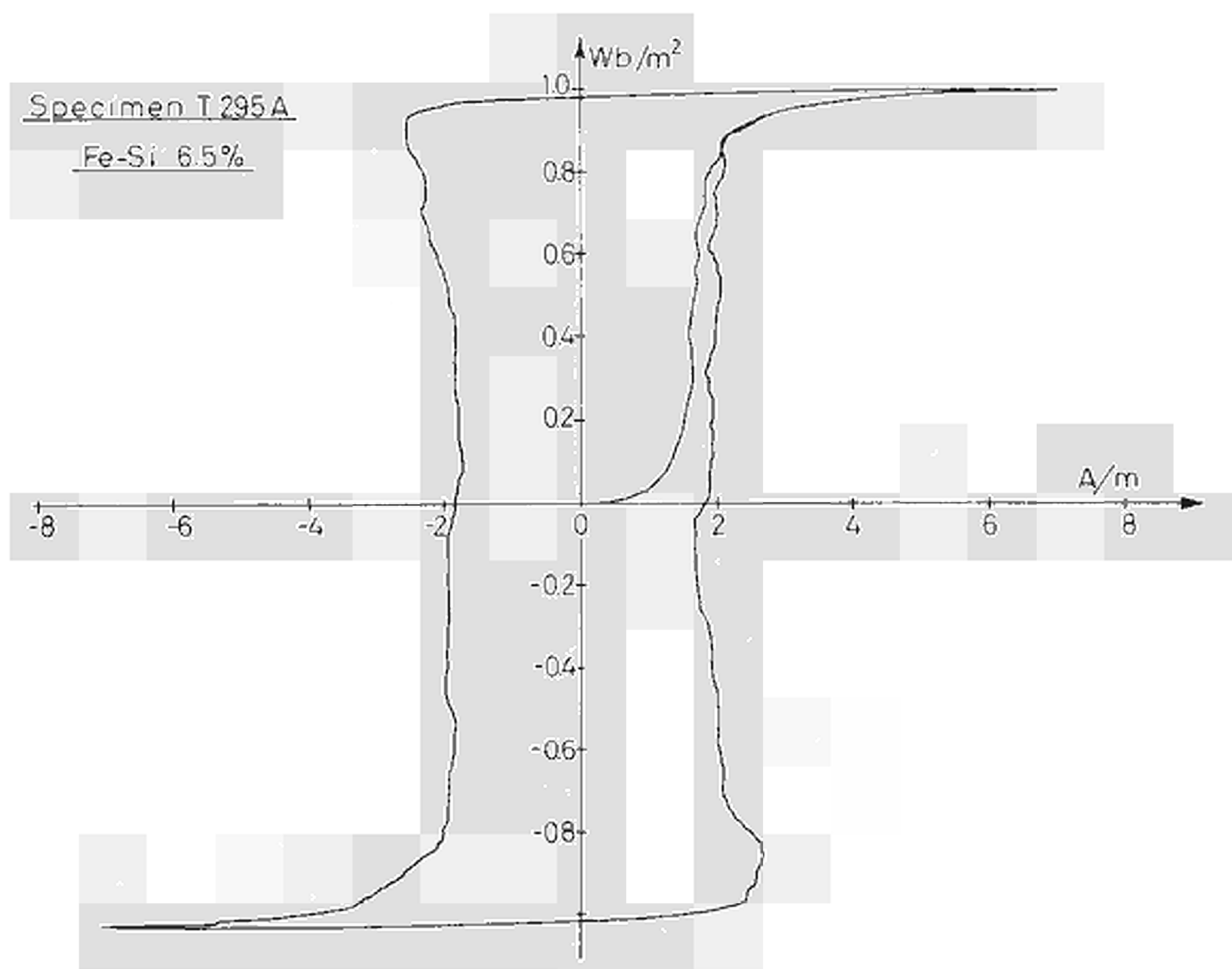


Fig. 2.4.1

Specimen T 295 A

Fe-Si 6.5%

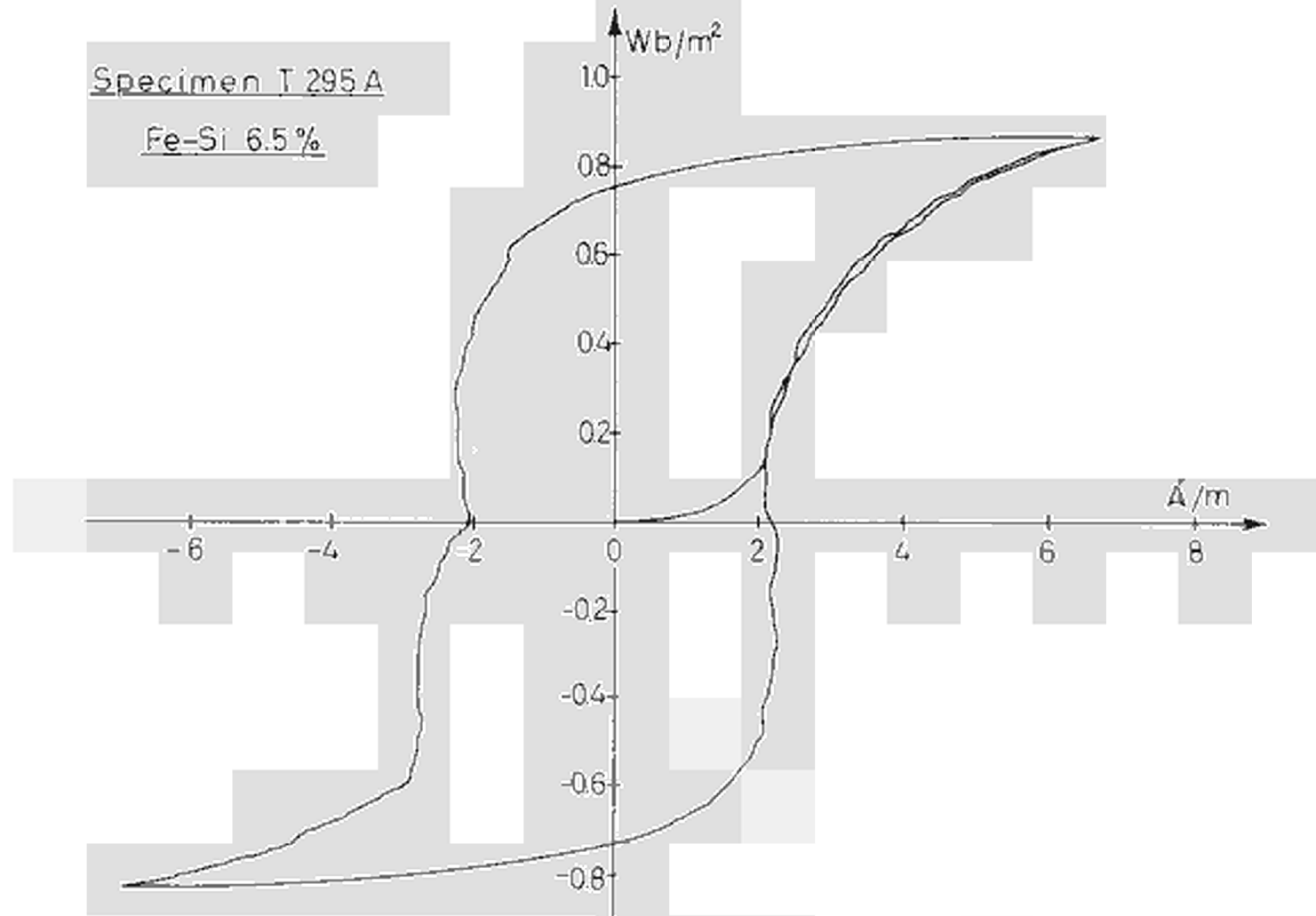


Fig. 2.4.2

Specimen T 295 A

Fe-Si 6.5%

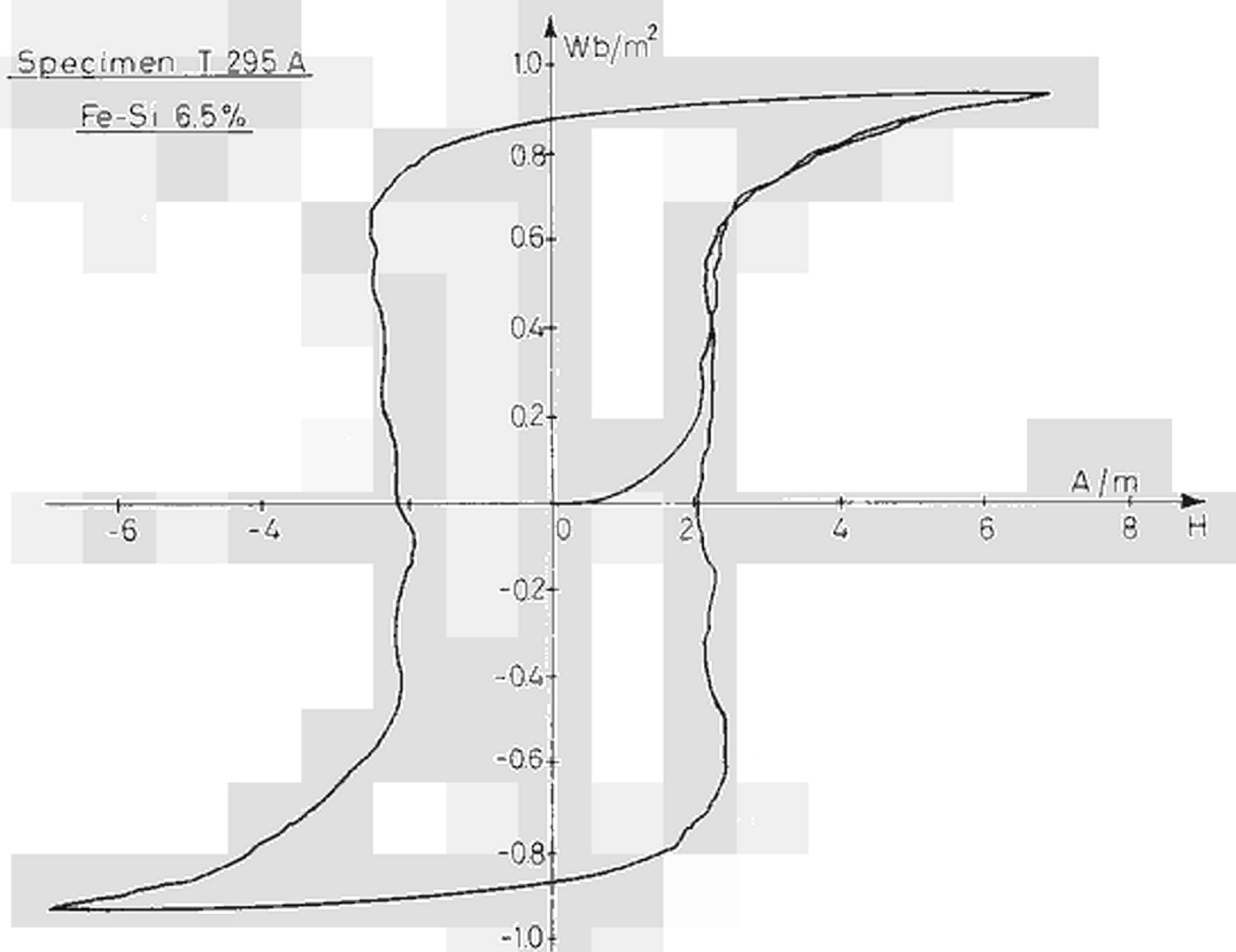


Fig. 2.4.3

Specimen T 295 A

Fe-Si 6.5%

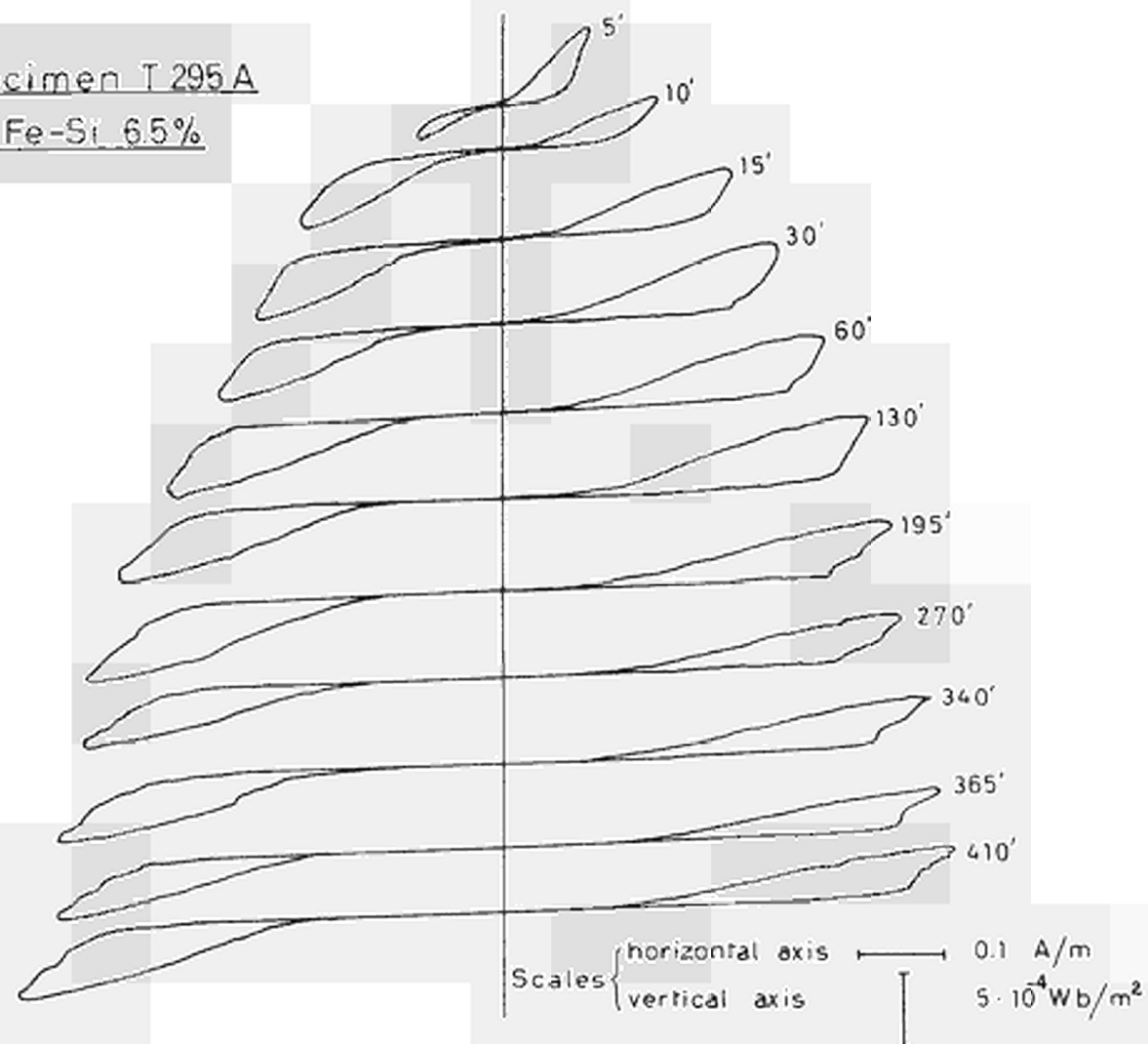


Fig. 2.4.4

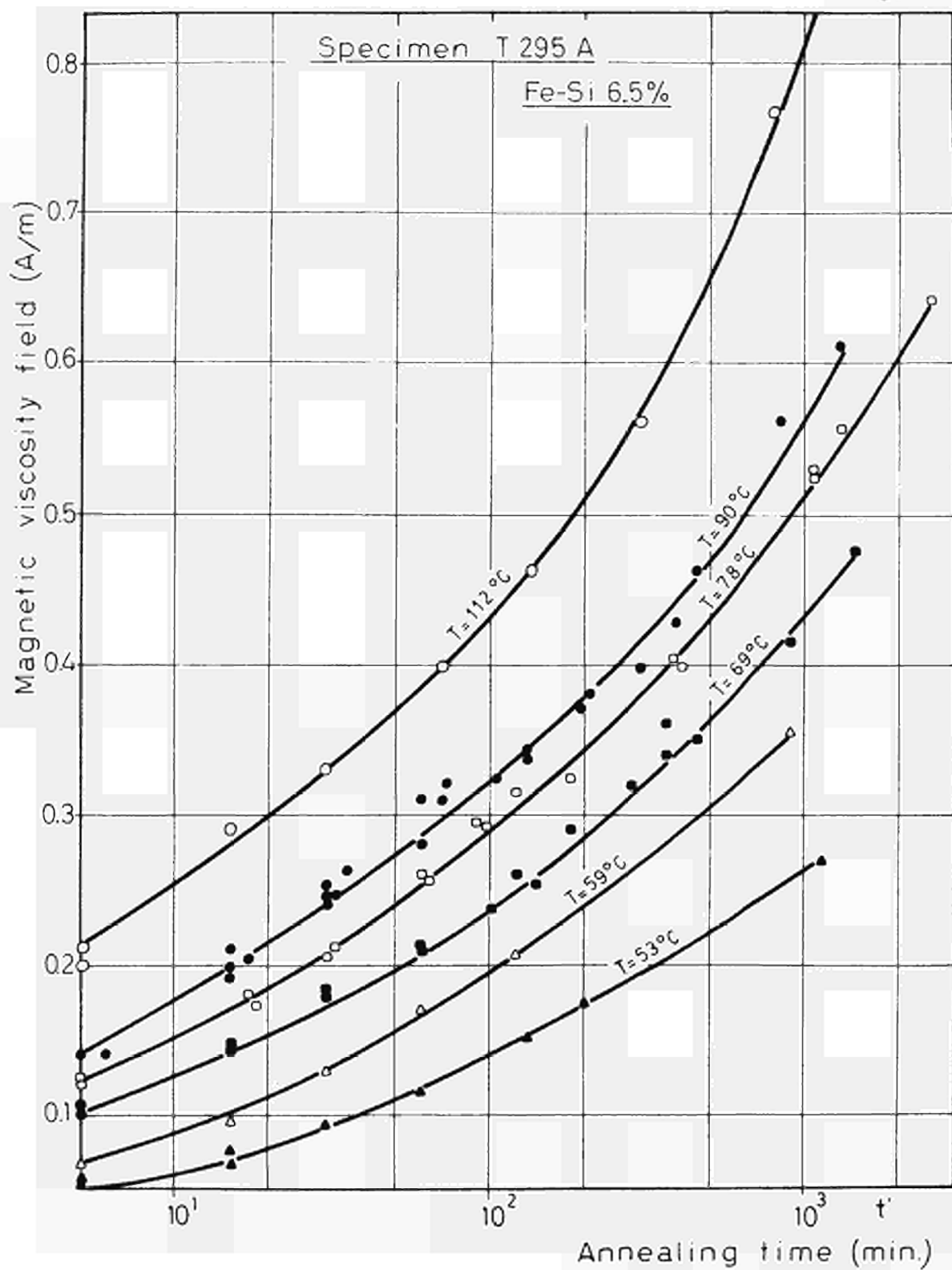


Fig. 2.4.5

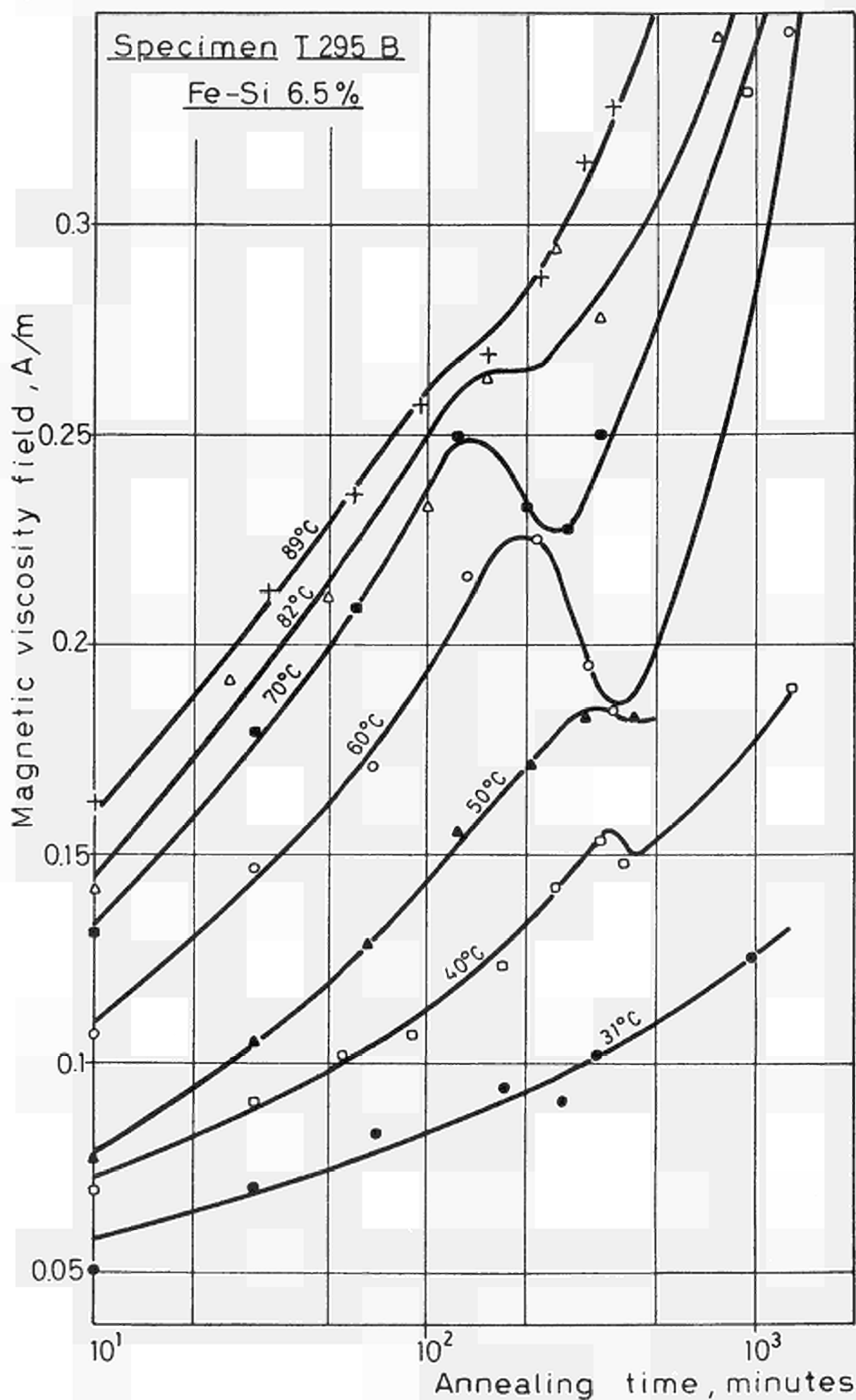


Fig. 2.4.6

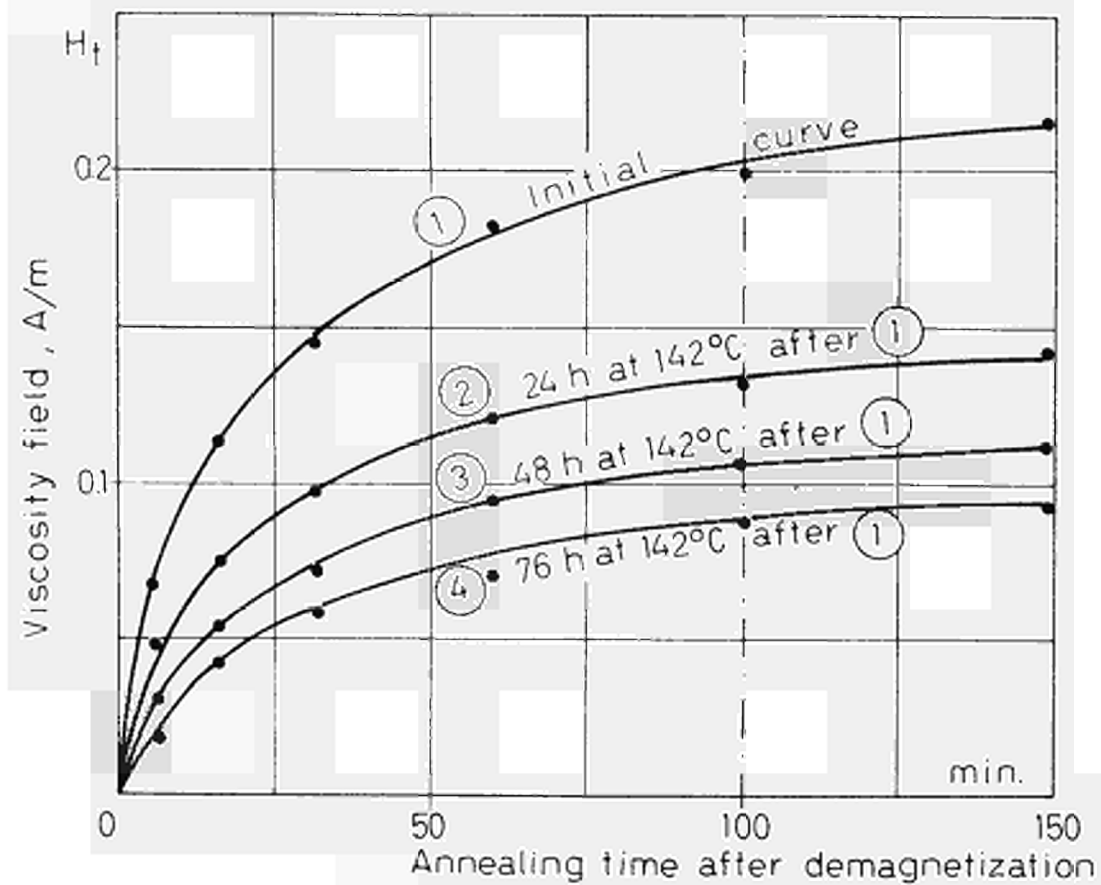


Fig. 2.4.7

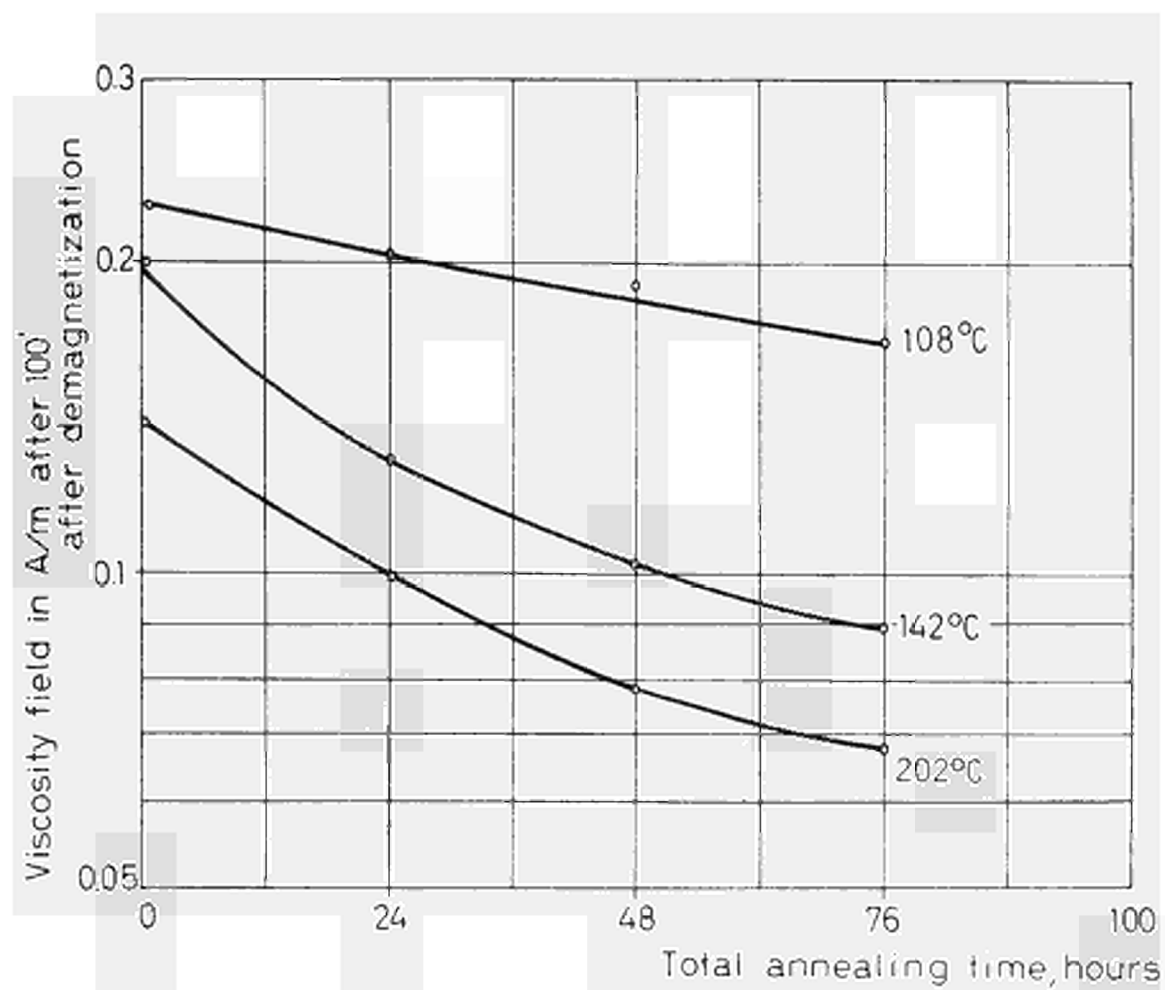


Fig. 2.4.8

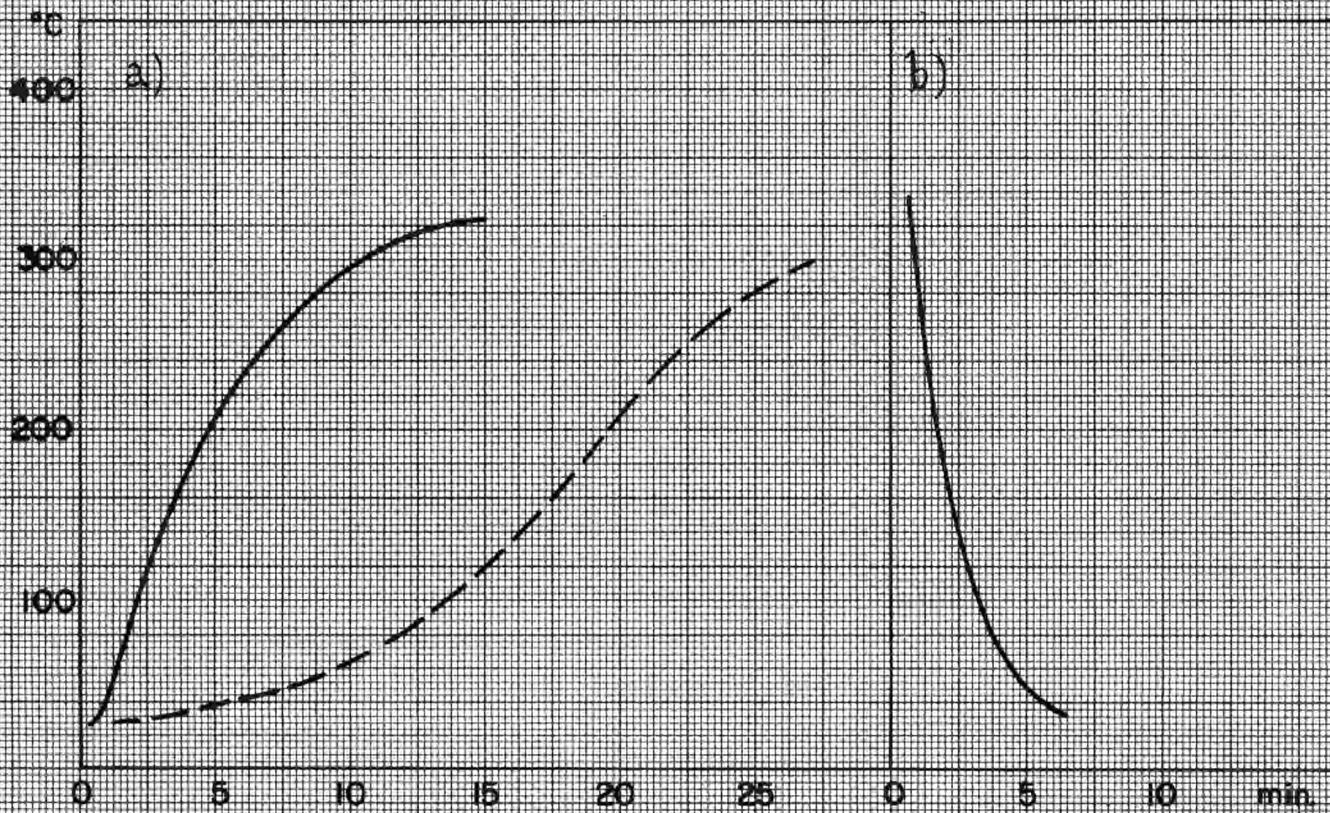


FIG. 2.6.3

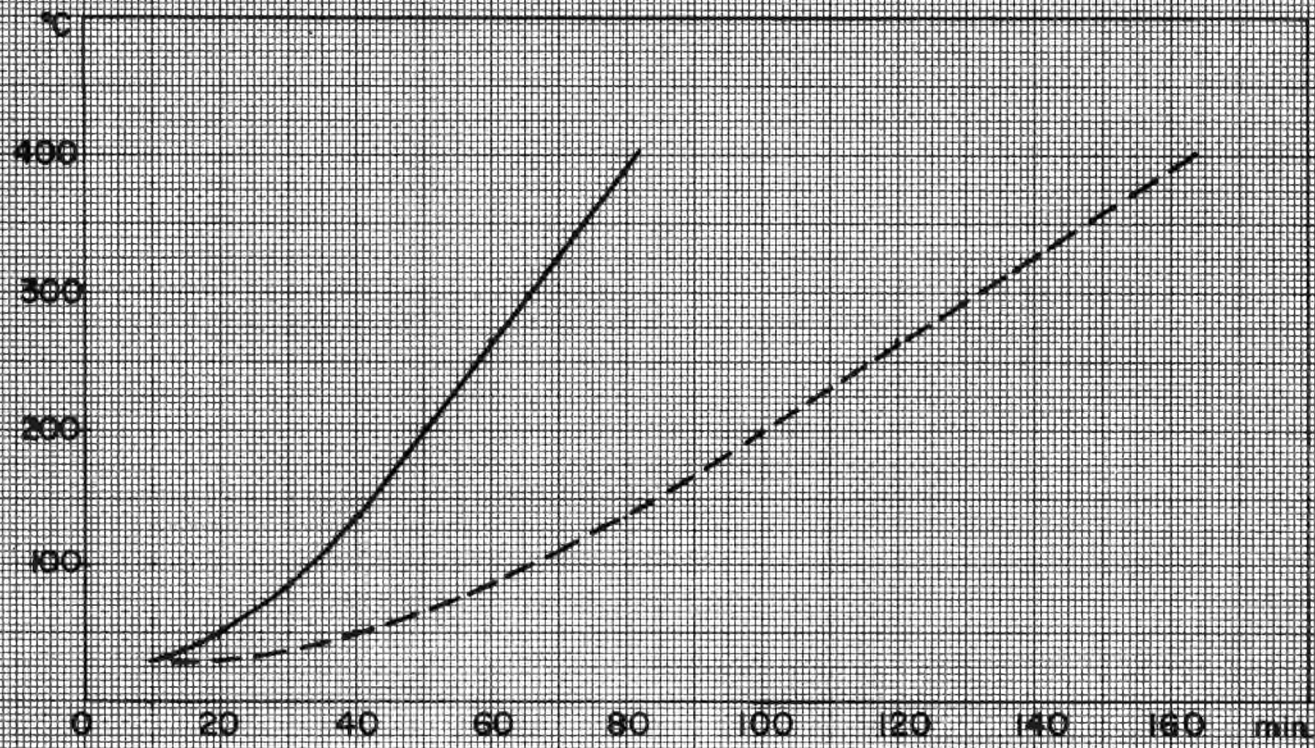


FIG 2.6.4

3. Neutron spectrum influence on the radiation damage of iron. (*)

As it is well known, the radiation damage production depends on the energy of neutrons; in a reactor environment the neutron energy spectrum is continuous and its shape varies with the location of the sample and with the composition of core and reflector.

Therefore in order to obtain an absolute value of the neutron dose effective for the damage production in a given material, it is necessary to know:

- a) the energy dependence of the damage production for the material under test;
- b) the shape and
- c) the magnitude of the neutron flux at the sample location.

This is not an easy task; first of all, in the case of iron, different damage models have been proposed, giving somewhat different energy dependence of damage and without definite experimental tests; no simple experimental method exists for measuring the spectral shape in reactors; the absolute value of the flux as obtained by activation detectors is affected by errors in the assumed spectral shape and in the activation cross sections.

These difficulties may justify the fact that often the dose has been evaluated with rough assumptions consisting in neglecting the energy dependence of damage, and in considering that only neutrons with energy above 1 MeV are effective and that the spectral shape is a pure fission one.

This first order approximation may be sufficient in some cases, but cannot be considered satisfactory from a general point of view; indeed the influence of the neutron spectral shape is predicted by any damage model and experimentally verified by Dahl and Yoshikawa (21).

Therefore in the frame of the present research it is intended to improve the dosimetry in order to obtain absolute values free, as far as possible, from errors due to spectral shape.

3.1. Outline to the problem approach.

(a) Energy dependence of damage production.

No research will be devoted to this subject, and the vacancy production cross section for iron proposed by Rossin (*) will be adopted, unless new data will become available during the course of the work.

(*) Work done in cooperation between IENGF (A. Ferro, G. Montalenti, G.P. Scardo) and SORIN (B. Chinaglia, R. Malvano, A.A. Rossi)

- (b) Measurement of the spectral shape and of the magnitude of the integrated flux.

A set of suitable threshold activation detectors may give a useful information about the spectral shape. The experimental procedure will consist in activating the detectors in the unknown flux and in a known reference flux; from the ratios of activities induced in the two irradiations it is possible to obtain the spectral deformation with respect to the reference flux. This procedure eliminates the greater part of uncertainties related to the absolute values of the cross sections. Because many of the reaction products are short-lived, it is not possible to irradiate the detectors inside the container of iron samples used for long term irradiations, because it can not be opened within a short time after the irradiation end.

Therefore a mock-up of the irradiation container has been built; part of this mock-up is shown in fig. 3.1.1. together with some detector foils.

The mock-up contains the same amount of iron as the samples and allows detector foils to be extracted within a short time after the irradiation end. The normalization between the short and long irradiations will be obtained by means of long lived monitory detectors ($\text{Ni}^{58}(n,p)$ and $\text{Fe}^{54}(n,p)$).

- (c) Magnetic and mechanical properties measurements on irradiated materials.

Dosimetry of neutron fluxes is usually performed by means of activation detectors. The change of mechanical, electrical or magnetic properties of suitable specimens with irradiation may eventually become another useful means to determine integrated neutron doses. Some ideas and some preliminary work done to relate and measure fluxes through the variations of magnetic properties with irradiation are now briefly outlined. This work is planned in close connection with standard activation detectors dosimetry and with similar experiments on the variations of mechanical properties as a function on neutron exposure.

Variations of magnetic properties with neutron irradiation were already investigated by Sery and Gordon (19) in a systematic study of several ferromagnetic alloys. Very strong variations of magnetic properties were in particular observed in Permalloy specimens, for which, moreover, the reciprocal of permeability was found to be a linear function of the fast neutron dose. The decrease of permeability can be associated to the formation in each domain of a uniaxially induced anisotropy energy. This energy is a function

of the number of displaced atoms and thus of the neutron dose. The relationship between amount of directional order which is created and number of atoms which are displaced seems, in this case, a relatively simple function of the dose, while this does not apply to the case of formation or destruction of long range order. In principle there is then the possibility to relate the measurement of the variation of the magnetic properties of permalloy type alloys to the absolute values of the neutron doses and, consequently, to the mechanical properties changes in iron specimens irradiated in the same conditions. Moreover, magnetic measurements are very sensitive and very easy to perform even on remotely located samples, so that one does not even need to remove the magnetic sample used as a detector from its position in the reactor and one can repeat measurements on the same sample during different stages of the irradiation. It must be pointed out that such measurements should prove useful even in the case of relative measurements of neutron doses.

The investigation will require several irradiations on suitable specimens with different neutron doses and different neutron spectra.

3.2. Specimens preparation for magnetic measurements

The work so far performed has concerned the preparation of specimens for magnetic measurements. A Permalloy type alloy (Fe 14%, Ni 75%, Cu 6%, Mo 4,5%, Mn 0,5%) was prepared by vacuum melting in the laboratory. The first results obtained were not completely satisfactory, and new alloy preparations will be necessary in the future. For the first specimens a commercially available Ultraperm alloy (Fe ~ 20%, Ni ~ 75%, Cr, Mo, Cu) manufactured by Vacuum Schmelze was used. Rings of 19 mm o.d., 13 mm i.d. were cut from foils 0.5 mm thick. The rings were annealed between 450°C and 600°C under a saturation magnetic field. Each sample is then formed by a set of 20 rings which are packed in aluminum holders suitable for easy handling. The holder section is shown in Fig. 3.2.1. Eighteen similar samples were prepared so far.

On each specimen the magnetization curve and hysteresis loop were measured by means of the electronic hysteresigraph. A typical set of measurements for one sample is shown in Figs. 3.2.2., 3.2.3. and 3.2.4. In Fig. 3.2.2. the hysteresis loop up to 1 Wb/m² induction value is traced. A part of the same loop around the axes origin is repeated with expanded field axis to show the coercive field value in a better scale.

In Fig. 3.2.3. the magnetization curve and hysteresis loop up to about 0.8 Wb/m^2 are shown from which μ_{max} turns out to be of the order of 360,000. Finally in Fig. 3.2.4. the initial part only of the magnetization curve and a Raleigh cycle are shown. The initial part of the magnetization curve is also repeated with expanded B scale, on the same figure. The same set of measurements were taken on all samples before irradiation.

3.3. Specimen preparation for mechanical properties measurement.

Miniaturized tensile specimens were prepared from Ferrovac E iron whose composition is reported in table 3.3.1. Heat treatments were identical to the cycles described in (1) for the fine grain materials. In the same time a set of Ferrovac E annular specimens have been also prepared to be used for microhardness tests. These specimens were radially tested (on twelve different radii) in order to know with a good precision the HV5 hardness number before irradiation and to compare the values with those obtained after irradiation.

Tensile specimens will be tested following the techniques described in point 2.1.b, while hardness tests should be useful to know the self shielding effect of iron either in tensile or in magnetic specimens.

3.4. Irradiation facilities and preliminary tests.

A peculiar irradiation container was designed and set up for this program. It was conceived in order to have a homogeneous irradiation of

- a) n° 6 toroidal specimens for magnetic measurements
- b) n° 60 tensile specimens and
- c) n° 12 annular specimens for hardness tests.

The irradiation container is reproduced in fig. 3.4.1 and fig. 3.4.2. The toroids have been inserted (with their terminals for connecting to the measure apparatus) in suitable aluminum holders (see figure 3.4.3.c) while hardness and tensile tests specimens are placed together in the same aluminum holder (see figure 3.4.3.: a, exploded view, b, open).

The radial distribution of tensile specimens and the hardness test position (on the top and on the bottom of the holder) were chosen to give a tool for evaluating any possible inhomogeneous distribution of the damage.

The holders were mechanically linked each other in order to obtain three self consistent bars which were placed in three aluminum tubes assuring a good refrigeration in the reactor.

The temperature distribution during the irradiation has been checked during an experiment with dummy specimens. The results are reported in figure 3.4.1. and in table 3.4.I. Through the actual irradiation the temperature will be only measured in the positions n° 5 and 6 (fig. 3.4.1.) in each tube and the data will be reported to the reference values obtained during the cited experiment.

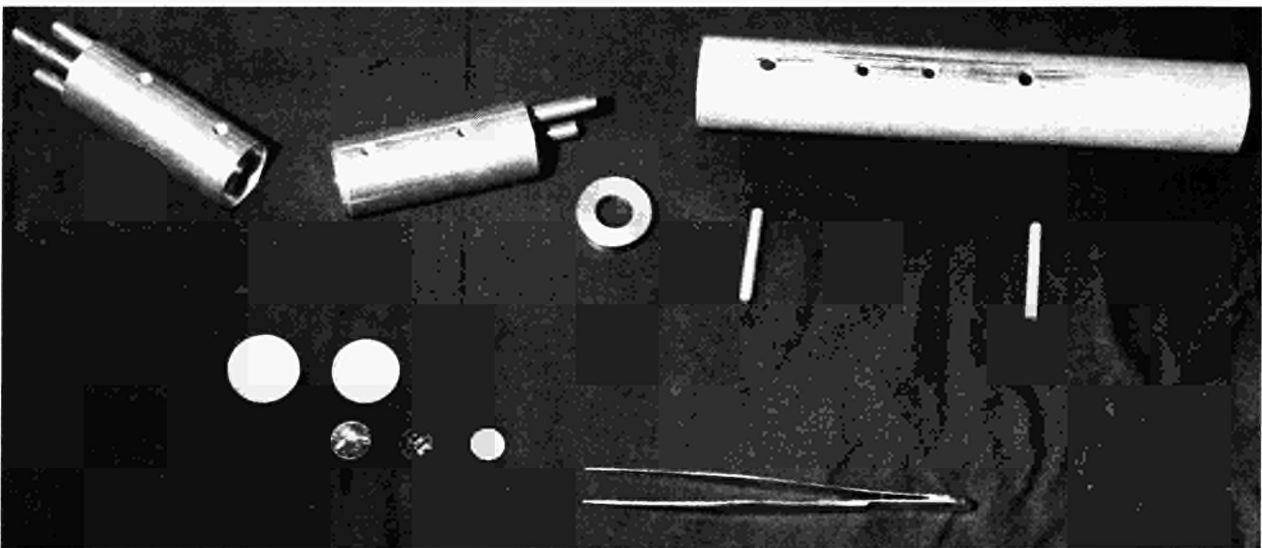


Fig. 3.1.1

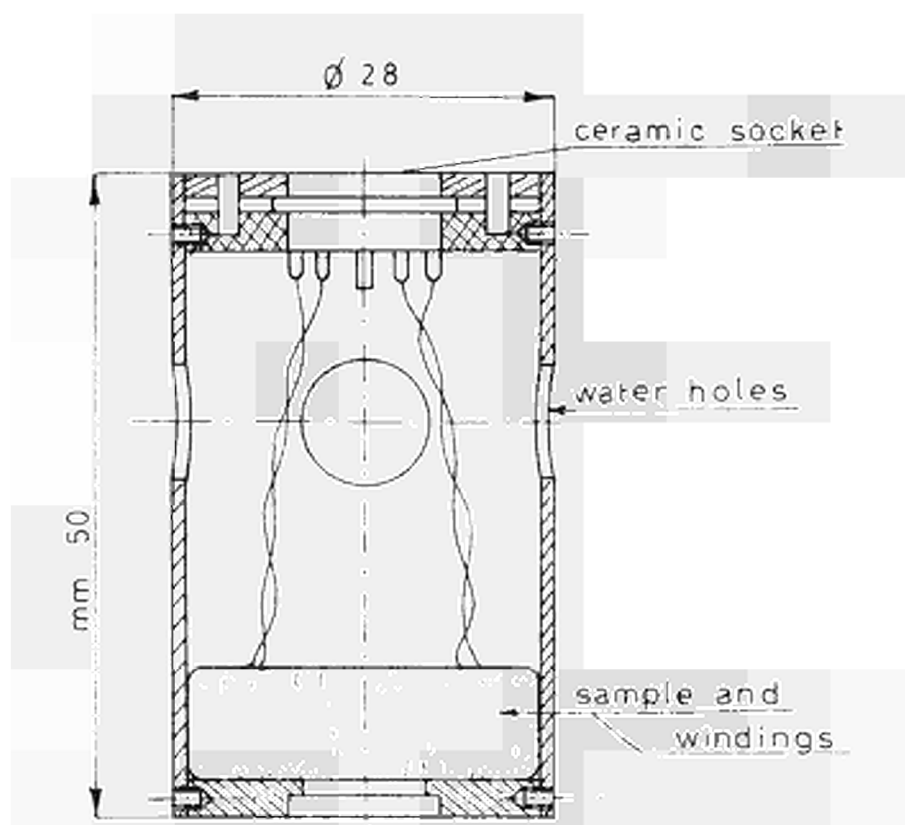


Fig. 3.2.1

Ultraperm specimen
before irradiation

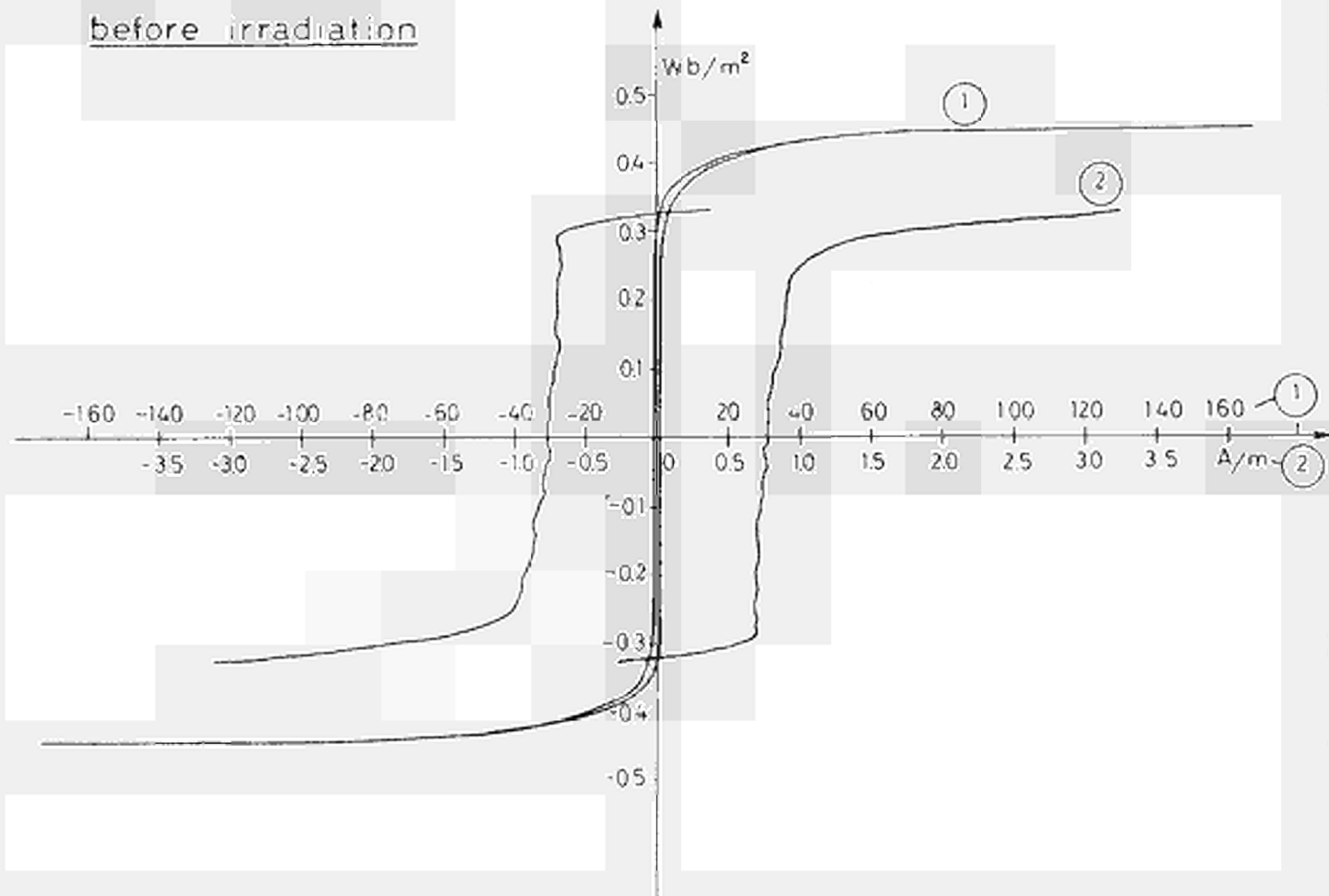


Fig. 3.2.2

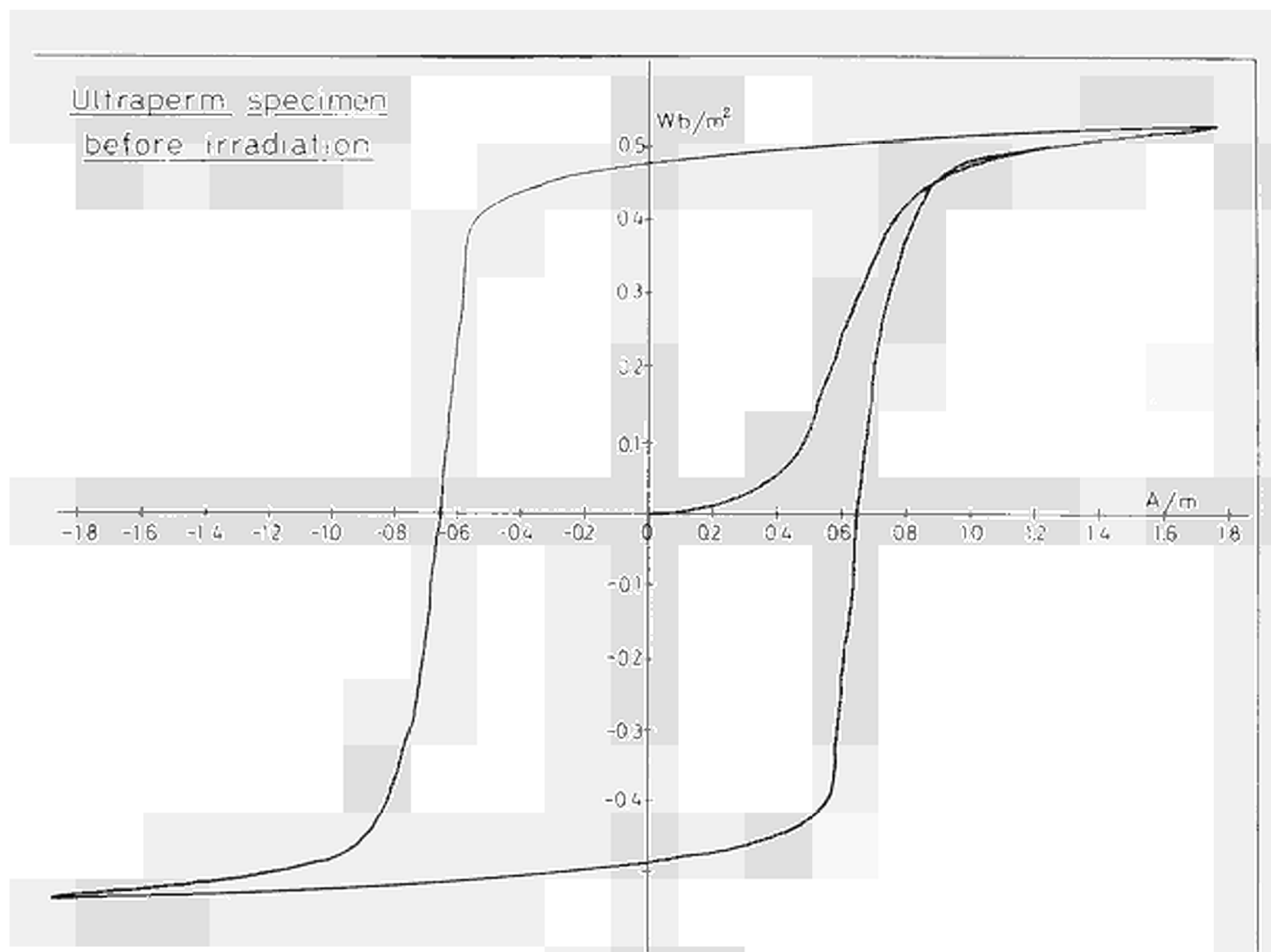


Fig. 3.2.3

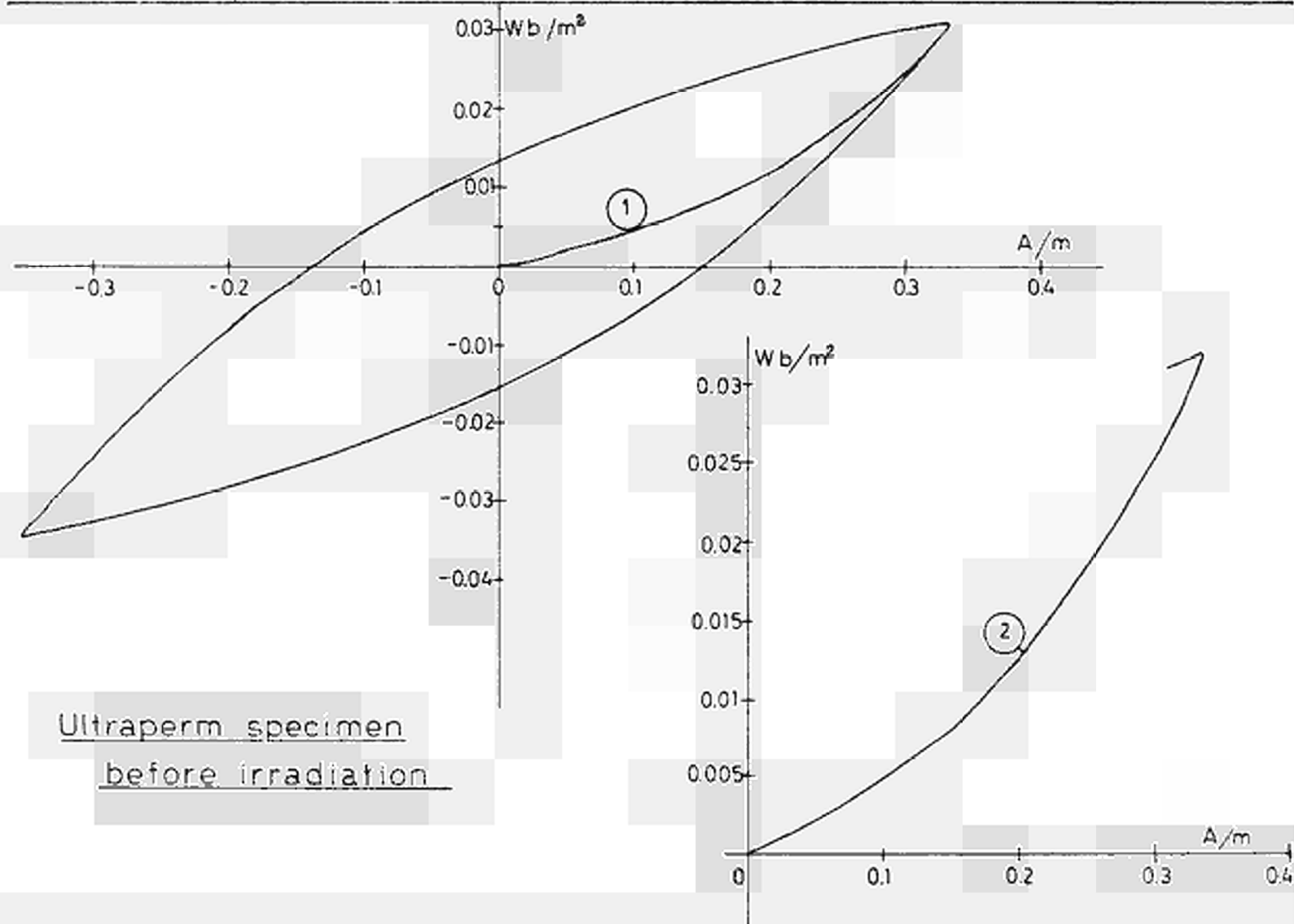



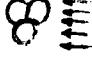

Fig. 3.2.4

TABLE 3.3.I

As furnished Ferrovac E composition in ppm; data quoted (⊗) are obtained by neutron activation analysis

Al (⊗)	As (⊗)	Co (⊗)	Cr (⊗)	Cu (⊗)	Mn (⊗)	Mo (⊗)	Ni (⊗)	V (⊗)	W (⊗)	P	C	N _{tot}
12,8	< 3	51,3	9,9	11	11,7	5,8	33	≤ 0,3	0,19	5	84	3

TABLE 3.4.I.

References	Measure positions	Temperature °C		
				
1	Anular specimen	32,5	30,5	30
2	Tensile spc	31	22	28
3	Tensile spc	31	29	30
4	Anular spc	34	32	32
5	Outer reference	30	28	28
6	Water inlet	26	26	26
7	Anular spc	34	32	32
8	Tensile spc	35,5	32	32
9	Tensile spc	35	31,5	32
10	IENGF toroidal	48	40	40
11	Anular spc	36	33	34
12	Outer reference	28	28	28

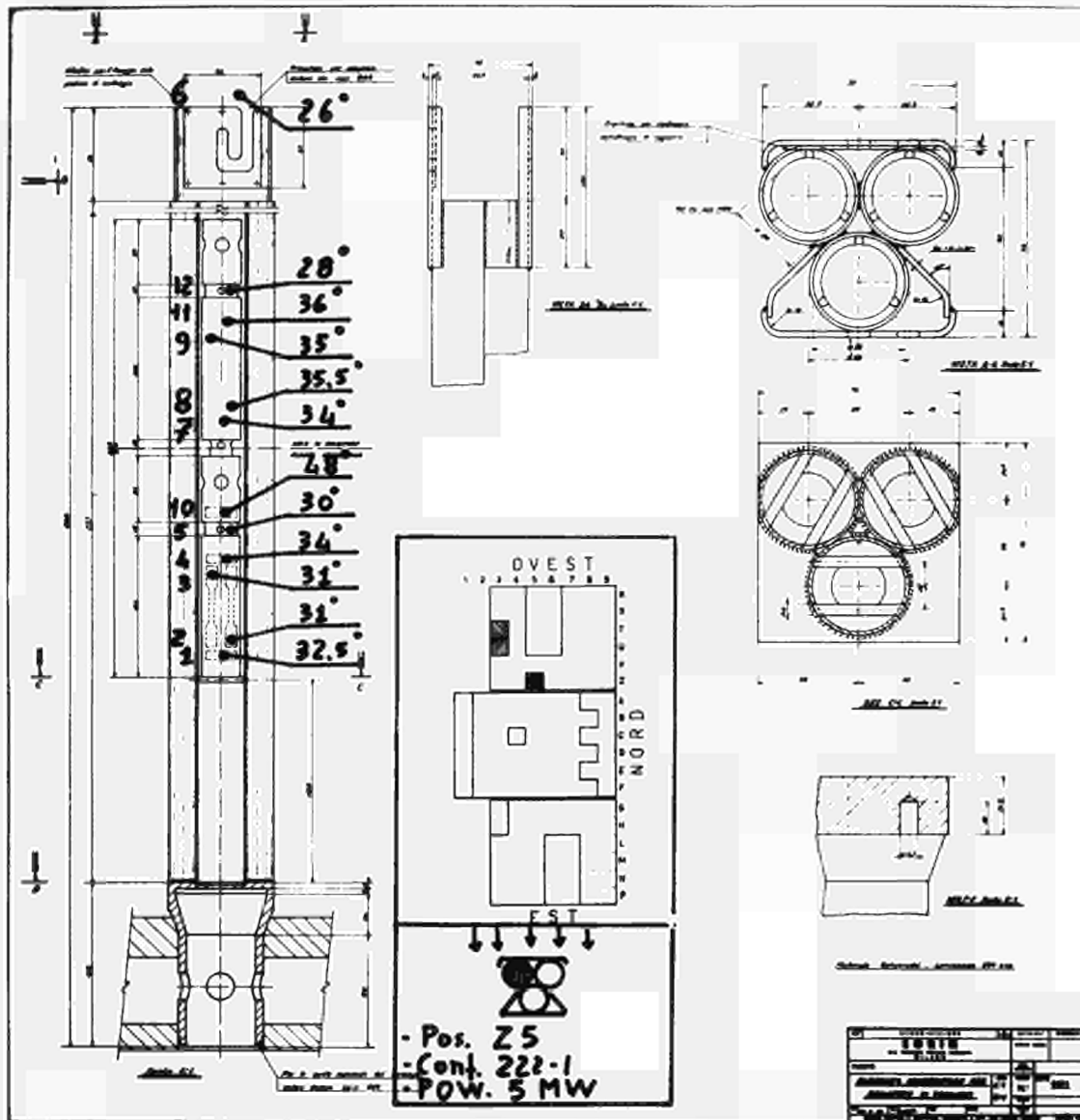


Fig. 3.4.1



Fig. 3.4.2

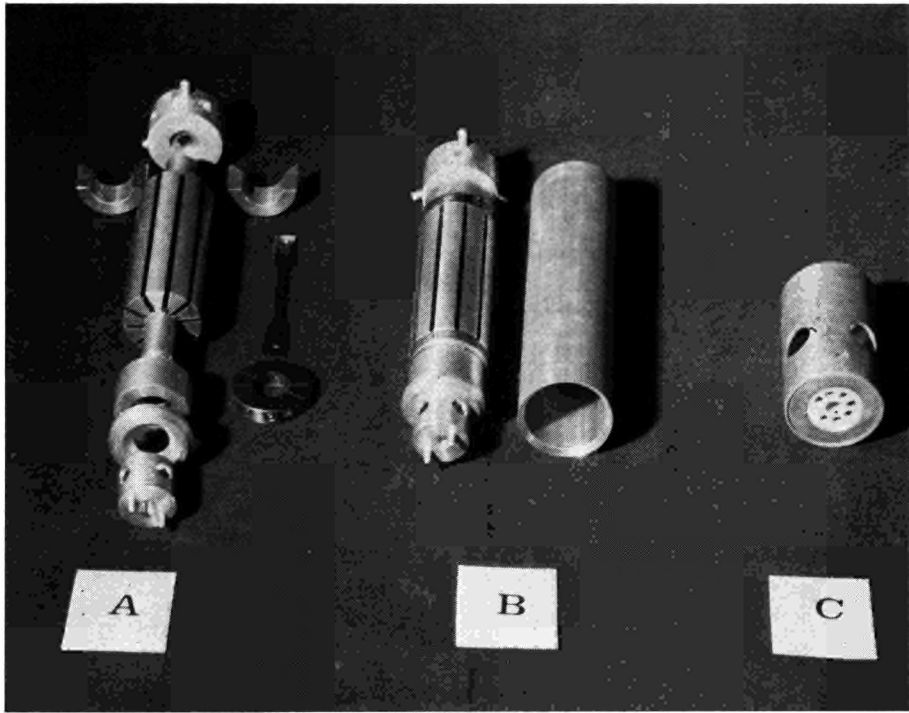


Fig. 3.4.3

4. Mechanical properties of some modified ASTM A212 steels.

As previously quoted (¹) a set of four ASTM A212 steels melts has been prepared with the addition of different killing elements ; their composition is reported in table 4.I. during some preliminary tests these materials were submitted to suitable heat treatments in order to prepare tensile specimens with different grain size. It was observed that if only the ferritic grains are counted, the Petch relationship cannot be fitted with the data obtained during tensile tests; possibly the equation might be applied if the perlitic grain size is also evaluated, but, at the present time, the problem does not seem to be of interest.

In the present report are summarized the results obtained in impact tests on specimens submitted to different heat treatment in order to obtain two slightly different grain sizes and to simulate the irradiation conditions. The materials structure after different heat treatments is also analyzed and some micrographies are reported.

4.1. Impact properties. (by F.S. Rossi, A.A. Rossi)

Ductile to brittle transition temperature was measured on sub-size V-notch specimens obtained from the four steels melts quoted in table 4.I. and treated according to the cycles described in table 4.1.I. The results are shown in figures 4.1.1. + 4.1.4.

The absorbed impact energy is about 10 kg.m/cm² for the steels killed with silicon or aluminum and passes to values higher than 15 kg.m/cm² when the steels are killed with titanium. The ductility appears to be dependent on the titanium concentration and the transition temperature, lower in the titanium killed steels than in the silicon and aluminum killed ones, seems to change with the titanium concentration. (See, for instance, the curves for the specimens C2 and D2 of identical grain size).

It should be also emphasized that the transition temperature for material D seems to be more grain size sensitive than for material C and, particularly, for materials A and B. This behavior, which should be carefully evaluated, has been ascribed to the different perlite distribution in the specimens structure (see below).

4.2. Microstructure. (by S. Appiano - M. Rossi)

Micrographic examinations have been done on a set of specimens suitably prepared from the four melts whose compos-

ition has been reported in table 4.I. Specimens were obtained from a \varnothing 20 mm rod rolled to square (10x10) mm section, annealed between 680 and 760°C for 15 h (pendular annealing) and slowly cooled. Sheets, 5 mm thick were obtained by cold rolling and specimens 50 mm long were cut from them. The specimens were austenitized for 20 min at 850°C then cooled and rapidly plunged in salt bath where they remained for times ranging from 2 sec to 15 h and then dropped into water. The surface of the specimen was polished and hardness was tested; micrographic examination was done on a section normal to the rolling direction.

Hardness data are reported in the diagram of figure 4.2.1. versus the soak time at 500, 600 and 700°C in the salt bath. Dotted lines refer to HRC numbers and the full lines to HRB numbers. The micrographs reported in figure 4.2.2. show the steels structure just before and after the beginning of the isothermal transformation and after a long permanence in the salt bath. Of particular interest are the titanium killed steels C and D; carbon is partially precipitated as TiC in the steel C which shows a structure richer in ferrite than A and B; steel D, containing Ti in excess, shows a completely ferritic structure.

The micrographs of the steels A and B show also that a shift of the TTT curves (isothermal transformation or Bain curves) is strictly dependent on the kind of killing element and would be taken in account during the heat treatment of those steels.

Some preliminary analysis of the nitrogen distribution in the different conditions have also been done, although not yet systematically; an exhaustive investigation in this field is now in progress.

TABLE 4.I

Type ASTM A212 B steels composition

	Al %	As %	Mn %	Si %	Ti %	S	P	C	N _{tot}	N _{prec.}
A	0,170	0,059	0,870	0,070	0,015	0,023	0,0168	0,335	0,0075	0,0073
B	0,025	0,065	0,750	0,145	0,012	0,022	0,0130	0,340	0,0088	0,0085
C			0,870	0,060	0,370	0,013	0,0085	0,310	0,0045	0,0044
D			0,900	0,080	1,020	0,015	0,0078	0,280	0,0046	0,0045

TABLE 4.1.I

Heat treatments of impact test specimens of ASTM A212 steels

N.	Treatment	Steels treated	Ferritic grain (mm ^{-1/2}) size (d ^{-1/2})
1	As furnished annealed steel cold rolled to (5 x 10)mm ² Mechanical cut - annealing 850°C for 3.5 h furn. cool. Notch cut	A 1 B 1 C 1 D 1	8.70 8.80 11.20 8.90
2	As furnished annealed steel cold rolled to (5 x 10)mm ² Mechanical cut - annealing 920°C for 3.5 h furn. cool. Notch cut	A 2 B 2 C 2 D 2	7.70 8.16 8.80 8.70
1 a	see treat. 1 then Annealing 950°C for 3.5 h 650° for 12 h furnace cooled annealing 1080°C for 3.5 h furn. cool.	A 1 a B 1 a C 1 a D 1 a	4.95 4 7.3 7.8
2 a	see treat. 2 then Annealing 950°C for 3.5 h 650°C for 12 h furn. cool. annealing 1080°C for 3.5 h furn. cooled	A 2 a B 2 a C 2 a D 2 a	4.9 4 7.3 7.8
1 bis	see treat. 1 then 11 days at 75°C + 13 days at 60°C	A 1 bis B 1 bis C 1 bis D 1 bis	
2 bis	see treat. 2 then 11 days at 75°C + 13 days at 60°C	A 2 bis B 2 bis C 2 bis D 2 bis	

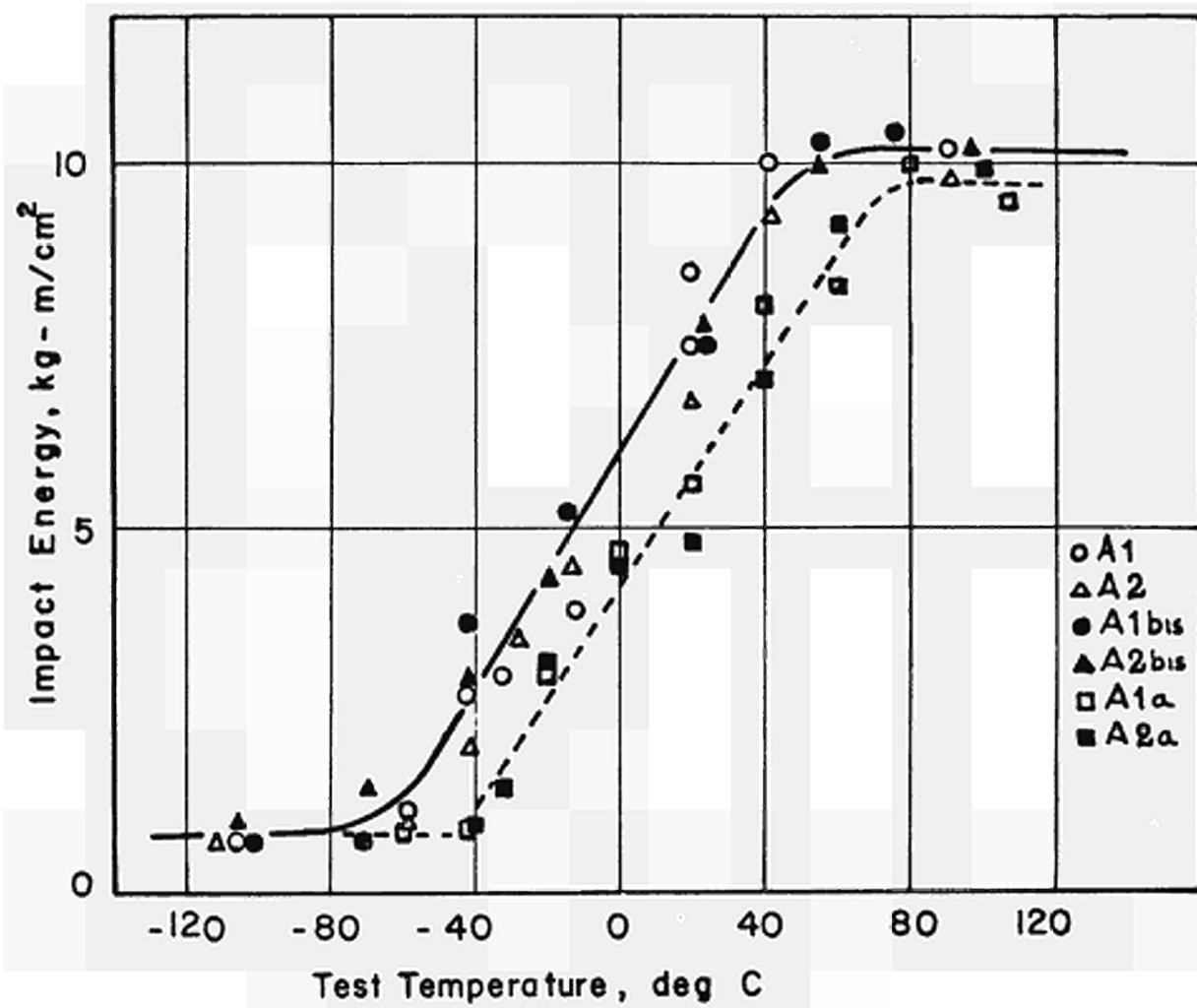


Fig. 4.1.1

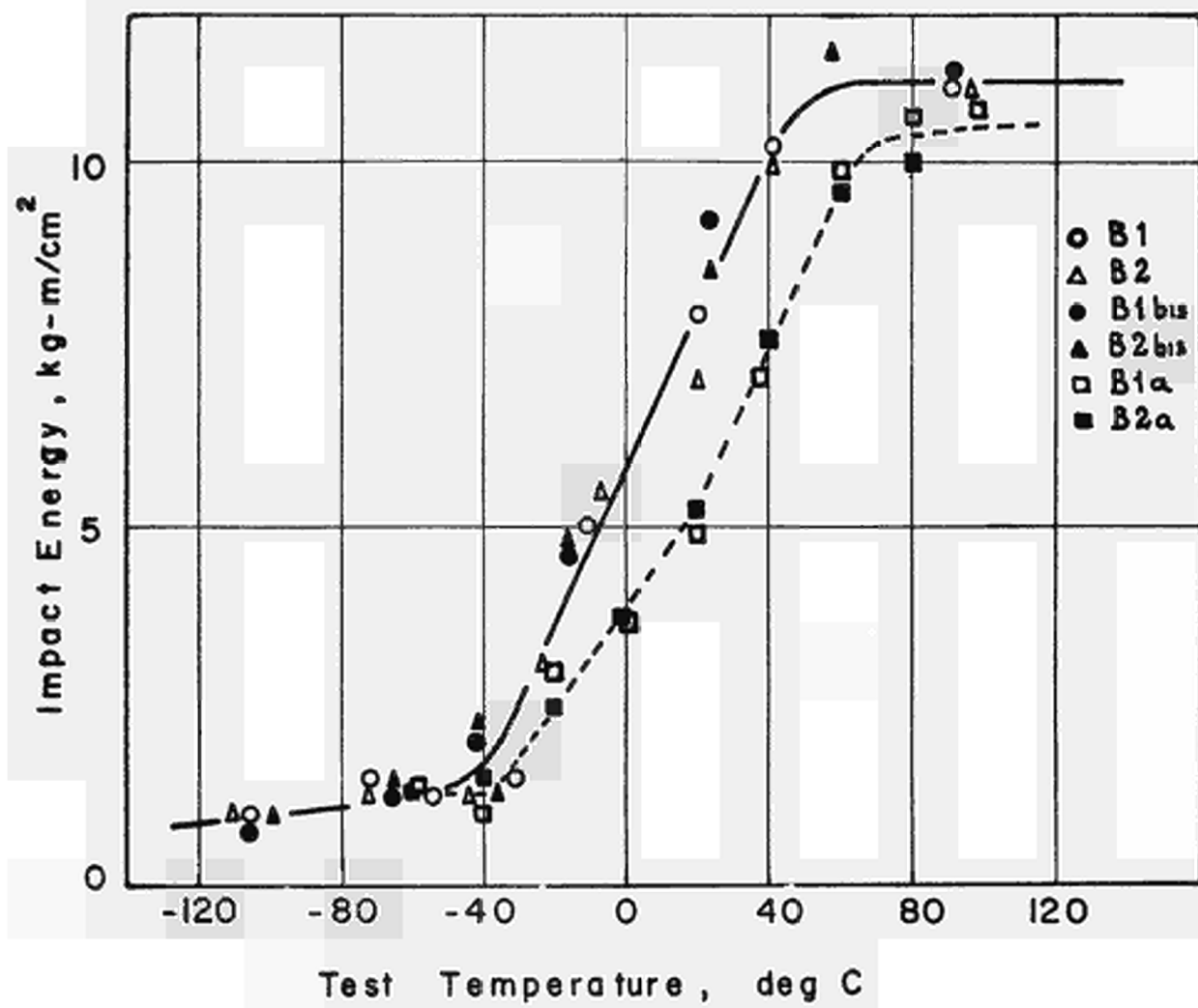


Fig. 4.1.2

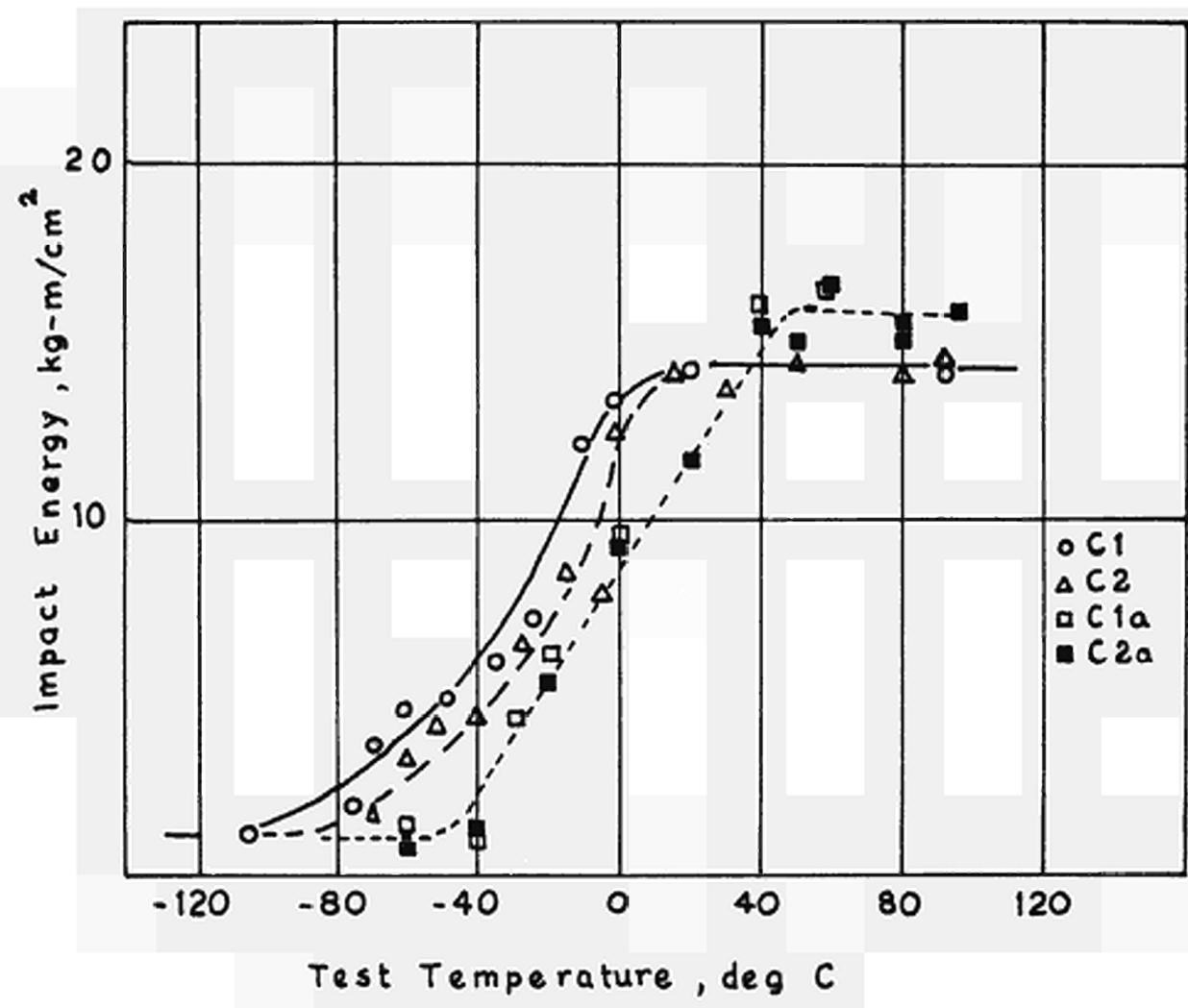


Fig. 4.1.3

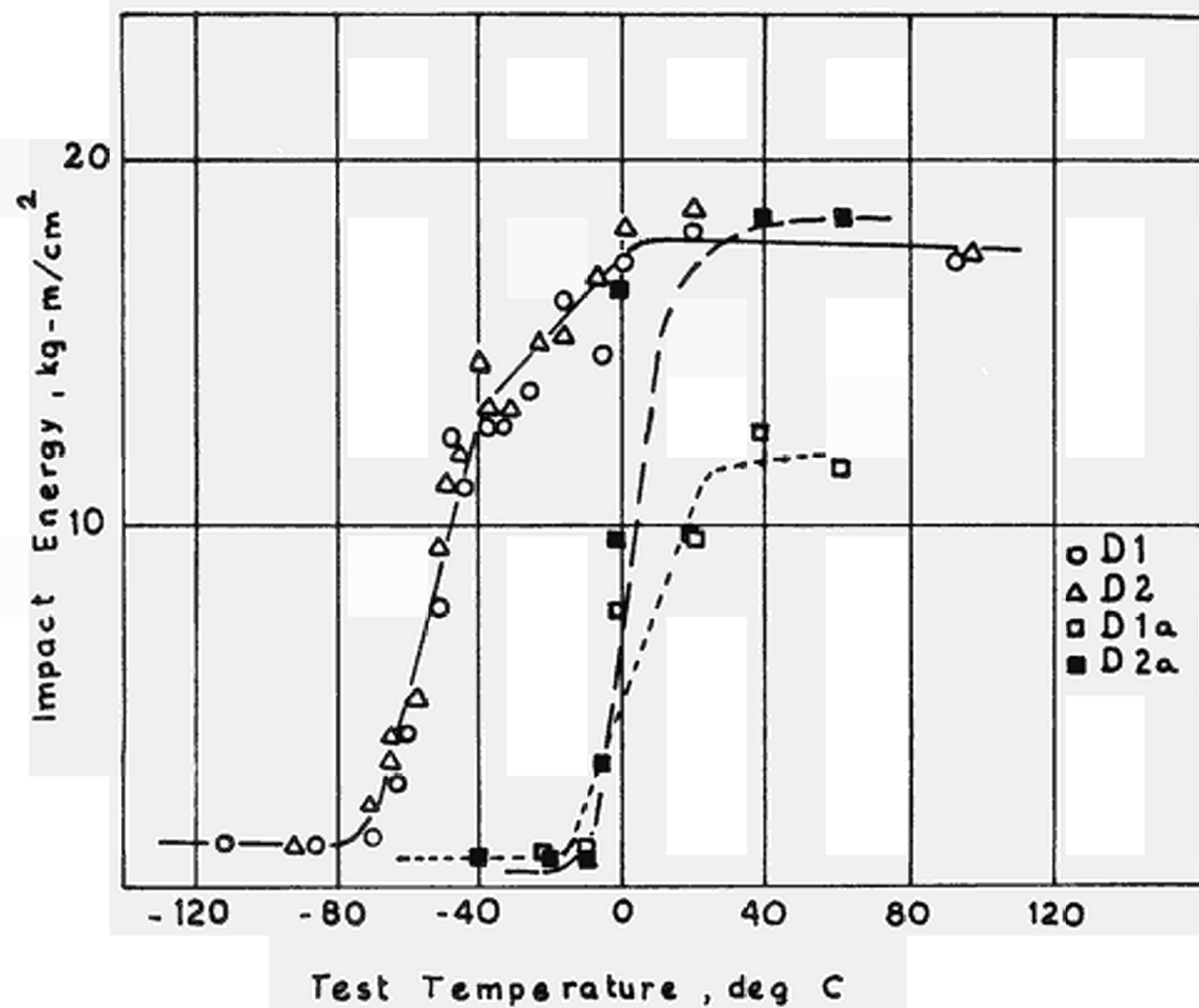


Fig. 4.1.4

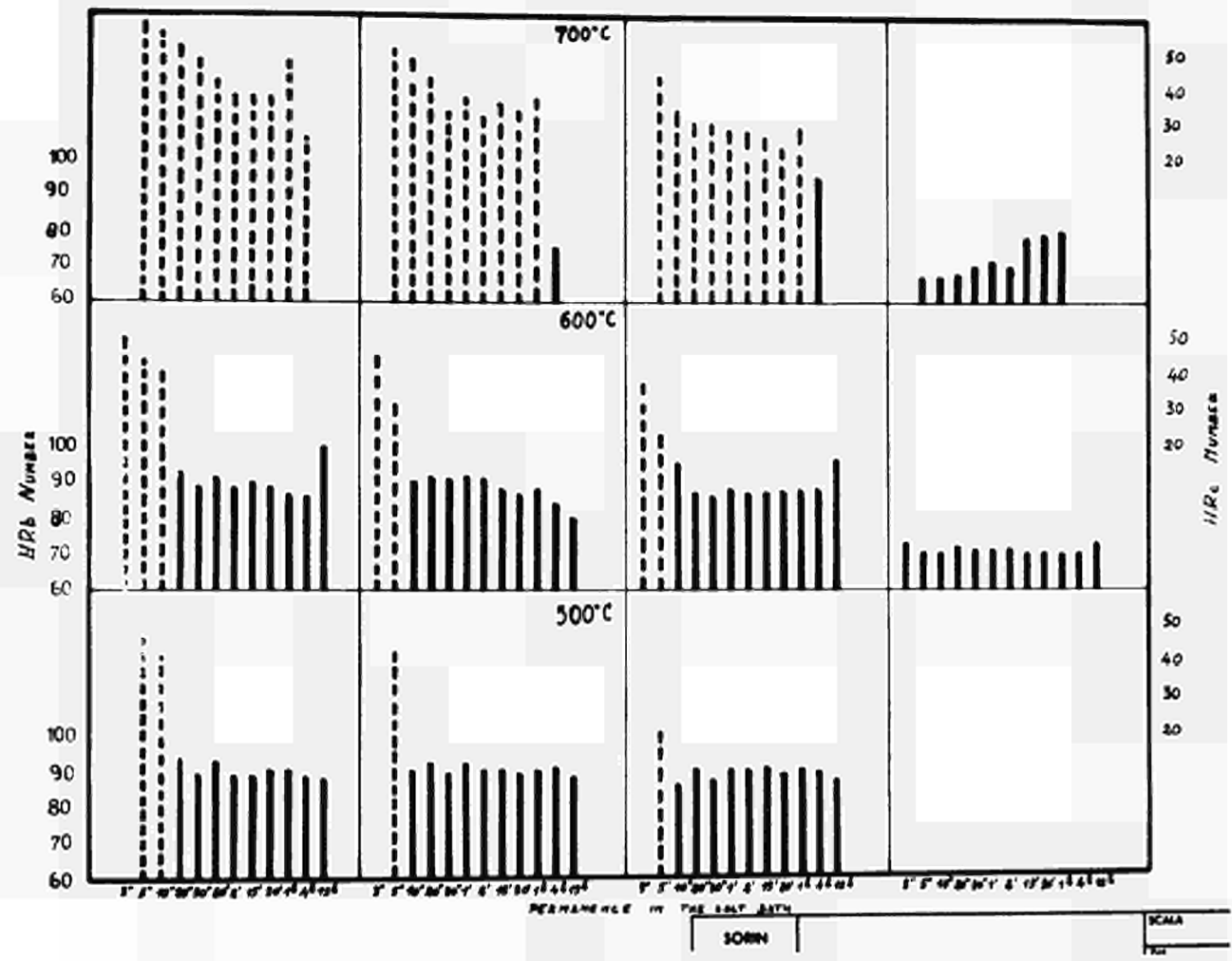


Fig. 4.2.1

Steel type A (Aluminium killed)

Salt bath temp. 500°C



permanence 5 sec
HRc 47

600°C



3 sec
50

700°C



5 sec
57



permanence 10 sec
HRc 41.5



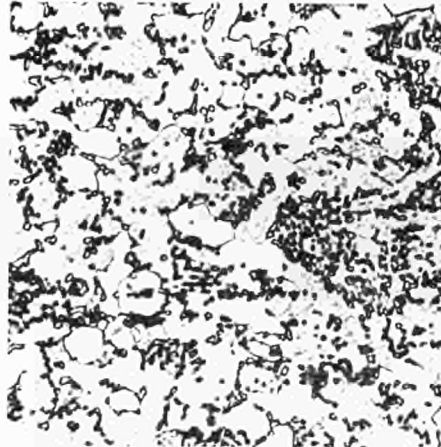
30 sec
HRb 89



15 sec
HRb 51



permanence 15 h
HRb 88



15 h
100



4 h
HRc 26

Fig. 4.2.2

Steel type B (Silicon killed)

Salt bath temp. 500°C

600°C

700°C



permanence 5 sec
HRc 47



3 sec
45



15 sec
42.5



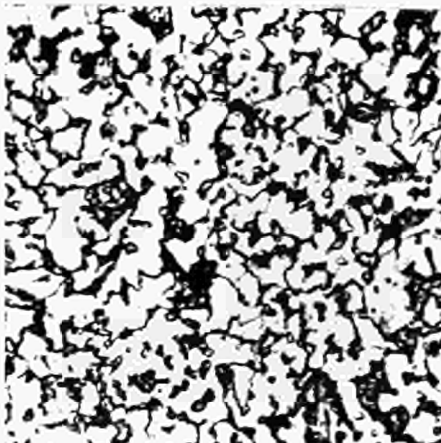
permanence 2 min
HRc 41.5



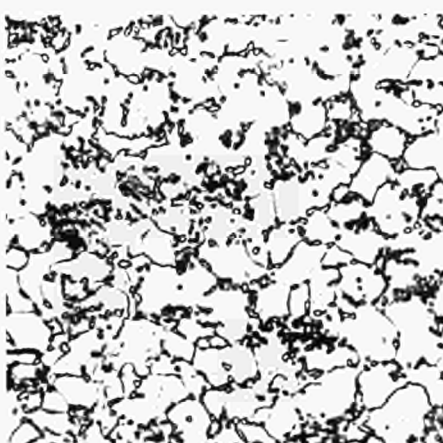
30 sec
HRb



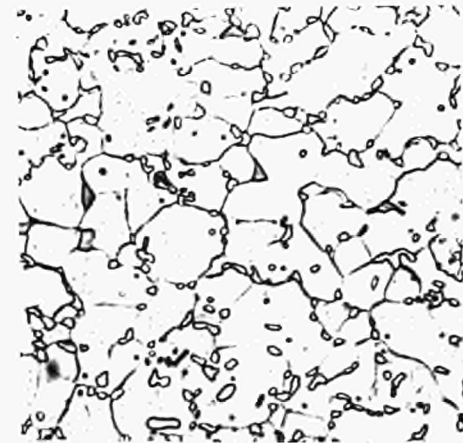
1 h
HRc 37



permanence 15 h
HRb 88



15 h
80



4 h
75

Fig. 4.2.2

BIBLIOGRAPHY

- (¹) F. ROSSI et al.: Influence of nitrogen in iron and steel under fast neutron irradiation. Final report. SORIN M/402 - febb. 1966.
- (²) M. CASTAGNA, A. FERRO, F.S. ROSSI, J. SEBILLE, G. SZABÓ MISZENTI : Mem.Sc.Rev. de Met. 63,6,1966, 555-561.
- (³) M. CASTAGNA, A. FERRO, F.S. ROSSI, J. SEBILLE: Paper n° 5 presented to the 69th ASTM annual meeting Atlantic City June-July 1966.
- (⁴) M. CASTAGNA, F.S. ROSSI, J. SEBILLE: Paper presented to the X^{ème} colloque de métallurgie du CEA - Saclay June 1966.
- (⁵) A.H. COTTRELL : Trans.Met.Soc. AIME 212, (1958)-192.
- (⁶) N.Y. PETCH : JISI, 1953, 25.
- (⁷) E.O. HALL : Proc. Phys. Soc. 64, 1951, 747.
- (⁸) M. CASTAGNA, R.L. COLOMBO, F.S. ROSSI, J. SEBILLE, G. SZABÓ MISZENTI : EUR Report n° 2322e, 1965.
- (⁹) D.B. CAMPBELL, J. HARDING in Response of Metals to high velocity deformations.Interscience publ.1961.
- (¹⁰) A.A. JOHNSON, N. MILASIN, EN.ZEIN - in Radiation damage in solids - IAEA 1962 - 277.
- (¹¹) A.S. WRONSKY, G.A. SARGENT, A.A. JOHNSON - ASTM STP 380, 1965, p. 69.
- (¹²) H. CONRAD, JISI 198-1961-p. 364.
- (¹³) G. HAHN, Acta Met., 10, 1962, p. 727.
- (¹⁴) H. CONRAD, W. HAYES, Trans. ASM 56, 1963, p. 125 and p. 249.

Steel type B (Silicon killed)

Salt bath temp. 500°C

600°C

700°C



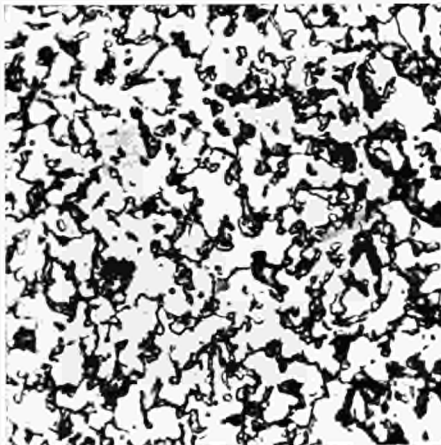
permanence 5 sec
HRc 47



3 sec
45



15 sec
42.5



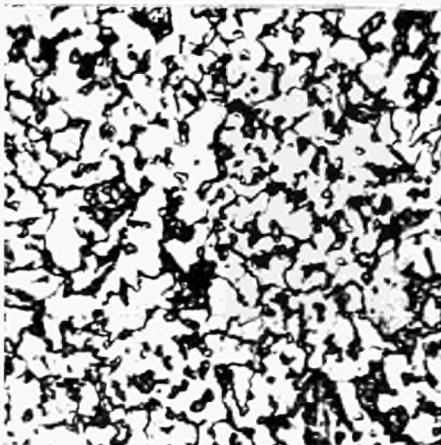
permanence 2 min
HRc 41.5



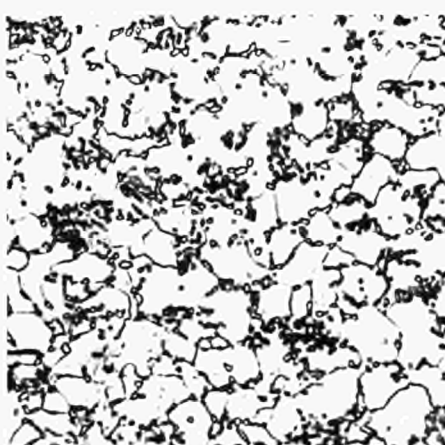
30 sec
HRb



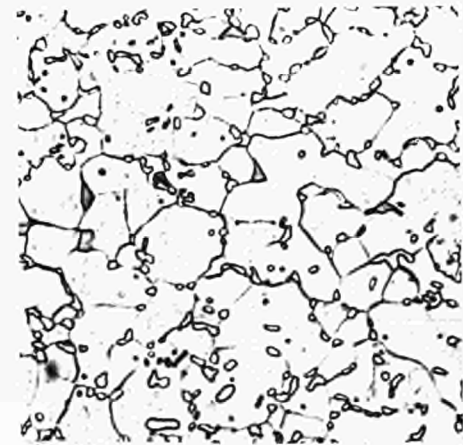
1 h
HRc 37



permanence 15 h
HRb 88



15 h
80

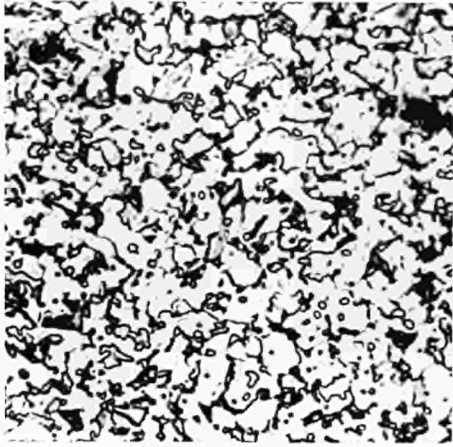


4 h
75

Fig. 4.2.2

Steel type C (0.3 Titanium killed)

Salt bath temp. 500°C



permanence 5 sec
HRc 20

600°C

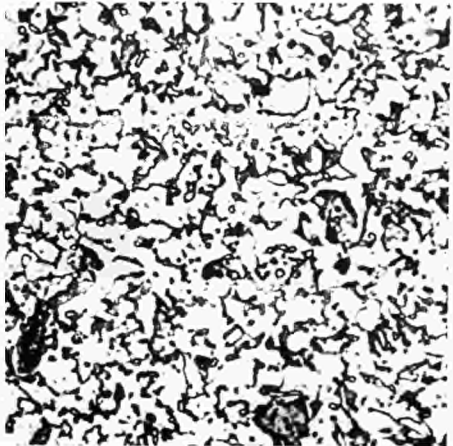


3 sec
39

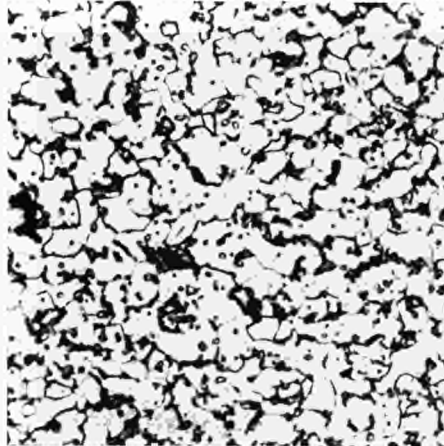
700°C



5 sec
43



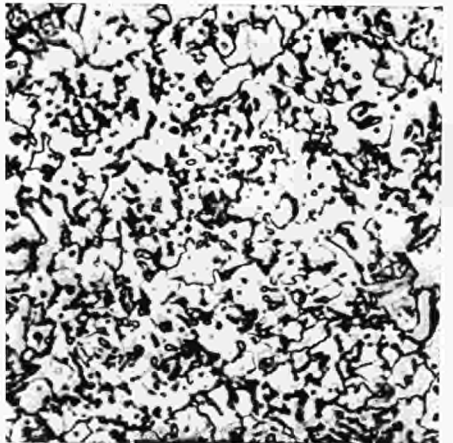
permanence 15 sec
HRc 90



20 sec
HRb 87



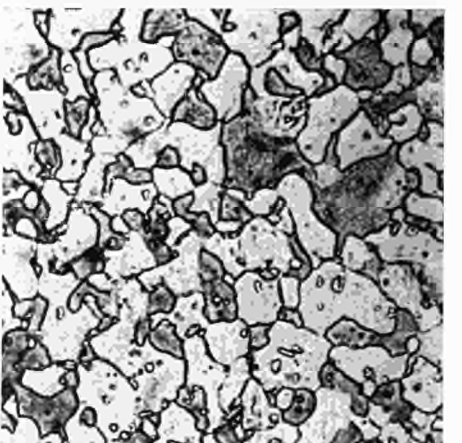
30 min
HRc 23



permanence 15 h
HRb 87



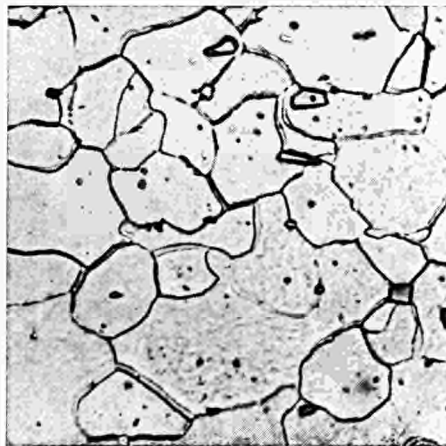
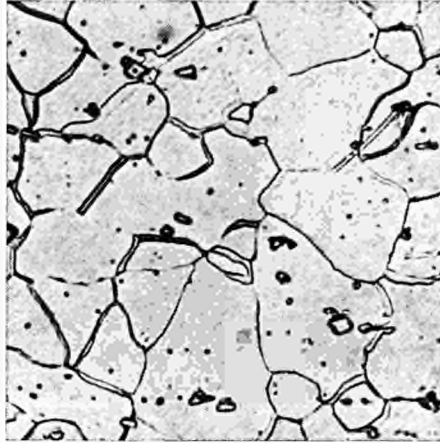
15 h
96



4 h
94

Fig. 4.2.2

Steel type D (1 % Titanium killed)
— annealed —



Type D steel structure does not change for quenching from 850°C

BIBLIOGRAPHY

- (¹) F. ROSSI et al.: Influence of nitrogen in iron and steel under fast neutron irradiation. Final report. SORIN M/402 - febb. 1966.
- (²) M. CASTAGNA, A. FERRO, F.S. ROSSI, J. SEBILLE, G. SZABÓ MISZENTI : Mem.Sc.Rev. de Met. 63,6,1966, 555-561.
- (³) M. CASTAGNA, A. FERRO, F.S. ROSSI, J. SEBILLE: Paper n° 5 presented to the 69th ASTM annual meeting Atlantic City June-July 1966.
- (⁴) M. CASTAGNA, F.S. ROSSI, J. SEBILLE: Paper presented to the X^{ème} colloque de métallurgie du CEA - Saclay June 1966.
- (⁵) A.H. COTTRELL : Trans.Met.Soc. AIME 212, (1958)-192.
- (⁶) N.Y. PETCH : JISI, 1953, 25.
- (⁷) E.O. HALL : Proc. Phys. Soc. 64, 1951, 747.
- (⁸) M. CASTAGNA, R.L. COLOMBO, F.S. ROSSI, J. SEBILLE, G. SZABÓ MISZENTI : EUR Report n° 2322e, 1965.
- (⁹) D.B. CAMPBELL, J. HARDING in Response of Metals to high velocity deformations. Interscience publ. 1961.
- (¹⁰) A.A. JOHNSON, N. MILASIN, EN. ZEIN - in Radiation damage in solids - IAEA 1962 - 277.
- (¹¹) A.S. WRONSKY, G.A. SARGENT, A.A. JOHNSON - ASTM STP 380, 1965, p. 69.
- (¹²) H. CONRAD, JISI 198-1961-p. 364.
- (¹³) G. HAHN, Acta Met., 10, 1962, p. 727.
- (¹⁴) H. CONRAD, W. HAYES, Trans. ASM 56, 1963, p. 125 and p. 249.

- (15) A. FERRO, G. MONTALENTI and G.P. SOARDO, to be published on the Proc.Caire Solid State Conf., Cairo 1966.
- (16) R.M. BOZORTH, "Ferromagnetism", Van Nostrand (1951) p.649.
- (17) P. MAZZETTI and P. SOARDO, Rev. Sci. Instr. 37, 548 (1966).
- (18) A. FERRO, P. MAZZETTI and G. MONTALENTI, Nuovo Cimento 23, 280 (1962).
- (19) R.S. SERY and D.I. GORDON, Navord Report 6127, June 1958.
- (20) A. FERRO, F.S. ROSSI, Paper presented to the 12th AIM Nat. meeting in Bari - Nov. 1966.
- (21) R.E. DAHL, H.H. YOSHIKAWA, Nucl.Sc. and Ing. 21, 312 (1965).
- (22) A.D. ROSSIN, Dosimetry for radiation damage studies, ANL 6826.

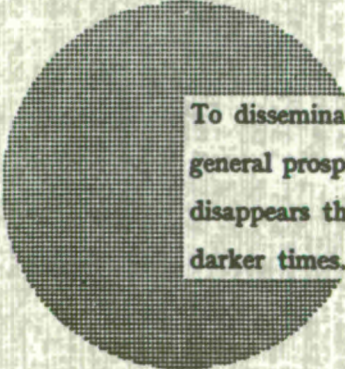
NOTICE TO THE READER

All Euratom reports are announced, as and when they are issued, in the monthly periodical **EURATOM INFORMATION**, edited by the Centre for Information and Documentation (CID). For subscription (1 year : US\$ 15, £ 5.7) or free specimen copies please write to :

Handelsblatt GmbH
"Euratom Information"
Postfach 1102
D-4 Düsseldorf (Germany)

or

Office central de vente des publications
des Communautés européennes
2, Place de Metz
Luxembourg



To disseminate knowledge is to disseminate prosperity — I mean general prosperity and not individual riches — and with prosperity disappears the greater part of the evil which is our heritage from darker times.

Alfred Nobel

SALES OFFICES

All Euratom reports are on sale at the offices listed below, at the prices given on the back of the front cover (when ordering, specify clearly the EUR number and the title of the report, which are shown on the front cover).

OFFICE CENTRAL DE VENTE DES PUBLICATIONS DES COMMUNAUTES EUROPEENNES

2, place de Metz, Luxembourg (Compte chèque postal N° 191-90)

BELGIQUE — BELGIË

MONITEUR BELGE
40-42, rue de Louvain - Bruxelles
BELGISCH STAATSBLAD
Leuvenseweg 40-42 - Brussel

LUXEMBOURG

OFFICE CENTRAL DE VENTE
DES PUBLICATIONS DES
COMMUNAUTES EUROPEENNES
9, rue Goethe - Luxembourg

DEUTSCHLAND

BUNDESANZEIGER
Postfach - Köln 1

NEDERLAND

STAATSDRUKKERIJ
Christoffel Plantijnstraat - Den Haag

FRANCE

SERVICE DE VENTE EN FRANCE
DES PUBLICATIONS DES
COMMUNAUTES EUROPEENNES
26, rue Desaix - Paris 15^e

ITALIA

LIBRERIA DELLO STATO
Piazza G. Verdi, 10 - Roma

UNITED KINGDOM

H. M. STATIONERY OFFICE
P. O. Box 569 - London S.E.1

EURATOM — C.I.D.
51-53, rue Belliard
Bruxelles (Belgique)

CDNA03321ENC